Role of deformations in the decay of $^{286}112$ formed in $^{48}Ca+^{238}U$ reaction

Dissertation submitted for partial fulfillment of the requirement for

The award of the degree of
Masters of Science
In
PHYSICS

Under
the supervision of
Dr. Manoj K Sharma

Submitted by
Kirandeep Sandhu
Roll no: 300804012

School of physics and Material Science
Thapar University
Patiala-147001 (Punjab)

Dedicated

To

My Parents

CERTIFICATE

This is to certify that Ms.Kirandeep Sandhu, Roll No.300804012 has worked on this dissertation report as a partial fulfillment for award of the degree of MASTERS OF SCIENCE in physics. I certify that the matter embodied in this report is of candidate's own record and not submitted to any other university in any part or full form for the award of such a degree.

(Dr. Manoj K Sharma)
Supervisor
SPMS, Thapar University
Patiala

Countersigned by:

Dr.O.P.Pandey
(Prof. & Head)
School of Physics and Material Science
Thapar University, Patiala

Dr.R.K. Sharma 21.2.10
Dean of academic affairs
Thapar University
Patiala

Acknowledgement

I owe my deepest gratitude to **Dr.Manoj Sharma**, *my worthy supervisor,* without him the dissertation would not have been possible. I thank him for his patience and encouragement that carried me on through difficult times, and for his insights and suggestions that helped to shape my research skills. I express my sincere thanks to him for his valuable guidance in caring out under his effective supervision, encouragement and cooperation. His visionary thoughts have influenced me greatly .His dynamical attitude has empowered me with zeal of energy to conquer the miner details of my research work.

I also thank **Dr.O.P Pandey, Professor** & Head, school of physics and material science for his support and providing facilities.

A special word of thanks to **Ms.Gudveen** , research scholar for the help and valuable suggestions whenever I need it out for her busy schedule.

Special thanks to all my friends and the staff at the school of physics and material sciences for providing me a friendly atmosphere and encouraging me throughout this work. I am deeply thankful to my family, their moral support and patient has bared fruit through completion of this thesis.

Kirandeep Sandhu

Roll No: 300804012
Date:

Abstract

In view of present day developments in the domain of nuclear physics, it is extremely important & essential to study the nuclear structure and related aspects at the extreme conditions of temperature, angular momentum, & energies in reference to the developments in theoretical & experimental nuclear physics. The tough challenges in nuclear perspective can be met only by developing and establishing clear understanding of related phenomena on the theoretical front, which could be utilized to plan and implement the predictions through experiments. A number of factors and properties influence the fusion-fission process and hence need to be handled with proper care in order to make meaningful predictions .One such aspect, which plays a significant role in fusion –fission process dynamics, is the role of deformed shapes of target, projectile and decaying fragments. It is therefore, important to account for shapes of target projectile combinations by considering proper deformation and orientation effects.

Keeping this in mind, we have investigated the role of deformations in ^{286}Uub nuclear system formed in ^{48}Ca+^{238}U reaction. The dynamical cluster decay model (DCM), with deformations upto hexadecapole deformations and 'compact' orientations included , is used to calculate the fusion evaporation residue cross-section for 3n and 4n emission in a hot fusion reaction at various incident energies ,taking proton magic number Z=126 and N=184 for super heavy region and DCM gives good description of measured fusion excitation function, $\sigma_{ER}(=\sigma_{3n}+\sigma_{4n})$ as a function of compound nucleus excitation energy E*, within one parameter fitting , the neck length ΔR(E*).Some interesting results related to nuclear fragmentation and their possible implications in reference to temperature and angular momentum effects are addressed in this work.

CONTENTS

Acknowledgement

Abstract

CHAPTER-1 INTRODUCTION PAGE NUMBER

CHATER -2 METHODOLOGY

List of figures

Introduction

We know in our modern periodic table there are two kinds of elements:

(a) Naturally Occurring Elements (b) Artificial Elements

Up to uranium 92, all the nuclei's are naturally occurring and beyond that all the nuclei's are artificial or man made which means that all of the transuranic elements (having atomic numbers greater than 92) are synthetic. Many of these elements have half lives that are comparable to the age of earth, which is about 4.5 billion years old. Since, 1940s, however, physicists have been able to produce unstable elements that decay to lighter elements on timescales that can range from thousands of years to tiny fractions of a seconds.

Now the question comes: How these elements beyond uranium were synthesized [1]: We must know that the number of elements in the periodic table come from the balance of two fundamental nuclear parameters, the strength of attractive nuclear force and repulsive attractive force [2]. In the synthesis process of heavy elements beyond uranium the neutrons are added to already existing elements which gets converted into next heavier element by undergoing β-decay process. In step by step process elements are added to our periodic table i.e. a neutron capture followed by β-decay can generate an element of periodic table with higher atomic number. Neutron capture can occur when neutron approaches a nucleus close enough for nuclear forces to be effective so that new isotope is unstable and it decays to emit electrons and neutrino via β-decay process. [1]

The way it works is this: we start out with a seed atom, say $_{26}Fe^{56}$. Suppose we are in a region of high neutron flux, so neutrons start to pile up on your atom. After you collect 6 neutrons, your atom becomes $_{26}Fe^{62}$, which is unstable to beta decay on a time scale (about 1 minute, in this case) shorter than the time between neutron captures. Before it can collect any more neutrons, it gets converted to $_{27}Co^{62}$ via β- decay, finally $_{28}Ni^{62}$ (a stable nucleus) is formed via subsequent β-decay. Now neutrons start to collect on the Ni, and so it goes, stepping through the periodic table.

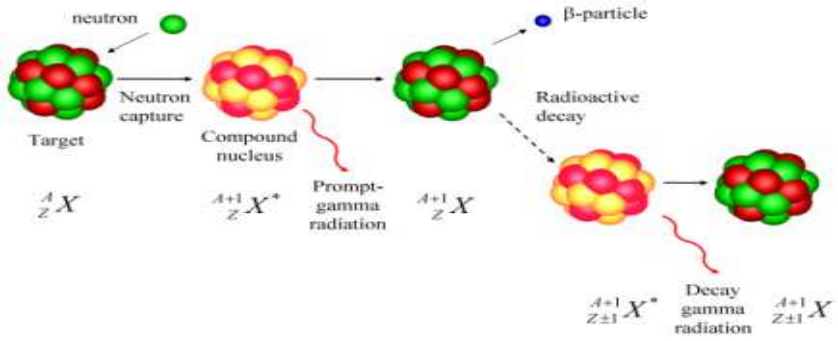

Figure 1.1, Compound nucleus formation via neutron capture and its subsequent decay via □-rays and β-particles.

Now as the no. of neutrons are constantly being added to heavy nuclei, so the heavy nuclei (whose atomic number is very high) might divide itself into new nuclei and the term fission comes into picture [2]. Fission can be spontaneous or it can be triggered via neutron or any other heavy ion. The liquid drop model can explain the formation of fission fragments and its possible implication for the synthesis of heavy/super heavy elements .Due to rapid increase in repulsive coulomb forces between the protons, the synthesis process gets limited by fission fragmentation.

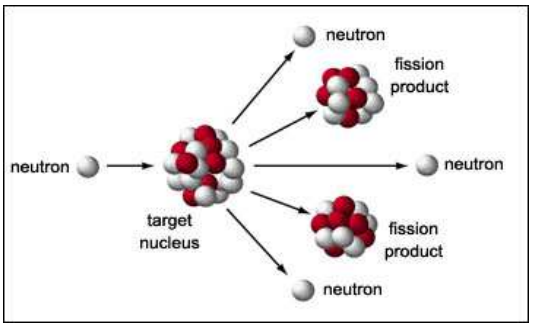

Figure1. 2 .Fission fragmentation along with emission of neutrons.

Now the liquid drop model tells us about fission fragments [3] and is a successful model to obtaining binding strength of composite nucleus .It treats the nucleus as a drop of incompressible nuclear fluid, first proposed by George Gamow and developed by Niels Bohr and John Archibald Wheeler. The fluid is made of nucleons (protons and neutrons), which are held together by

the strong nuclear force. This model however does not explain all the properties of the nucleus, but does explain the spherical shape of most nuclei along with decent prediction binding energy of the nucleus. The liquid drop formula reads as:

$$E_B = a_V A - a_S A^{2/3} - a_C \frac{Z(Z-1)}{A^{1/3}} - a_A \frac{(A-2Z)^2}{A} + \delta(A,Z)$$

Mathematical analysis of the theory delivers an equation which attempts to predict the binding energy of a nucleus in terms of the numbers of protons and neutrons it contains. This equation has five terms on its right hand side. These correspond to the cohesive binding of all the nucleons by the strong nuclear force, the electrostatic mutual repulsion of the protons, a surface energy term, an asymmetry term (derivable from the protons and neutrons occupying independent quantum momentum states) and a pairing term (partly derivable from the protons and neutrons occupying independent quantum spin states).

It is important to note that nuclei can survive beyond macroscopic limit (due to liquid drop model) into transuranium region where necessary balance between nuclear force and Coulomb force is achieved by Shell stabilizations. [5]

According to the concept of shell stabilizations: Systematic measurements of the binding energy of atomic nuclei show systematic deviations with respect to those estimated from the liquid drop model. In particular, some nuclei having certain values for the number of protons and/or neutrons are bound more tightly together than predicted by the liquid drop model. These nuclei are called singly/doubly magic [5]. This observation led scientists to assume the existence of a shell structure of nucleons (protons and neutrons) within the nucleus, like that of electrons within atoms. And as stepping towards the higher elements, strong electrostatic repulsion that drives protons apart, for nuclei with more than 104 protons the repulsive Coulomb forces are so strong that they should prevent the binding of the neutrons and protons in the nucleus. That's why predication about the binding energies from liquid drop model is not sufficient to tell about the stability of heavy and super heavy elements. But experiments performed in Germany, Japan, and Russia have bolstered theories that the lives of nuclei become longer as certain configurations of protons and neutrons are achieved i.e. stabilizing effect is

created by the arrangement of the nucleons on discrete energy levels (shells) which enables the existence of even heavier nuclei. All elements with Z>104 exist merely due to these "shell effects and the term super heavy elements came in existence near the next (predicted) double shell closure above Lead (Pb).i.e.at Z=126, N=184, shape along with other possibility Z=114,120 and N=184.Hence for these closures super heavy name was coined [6].

In general elements with Z>104 i.e. Rutherfordium of Transactinide series are considered as the super heavy elements. Now, the question arises why we start considering super heavy elements from Rutherfordium: [2]

In traditional form the word super heavy elements taken to be the synonym of the elements which exists due to their nuclear shell effects and which means high stabilities. Similarlaly rutherfordium isotopes also very stable and shell effects are observed in Rutherfordium. So super heavy elements and transactinide elements shares equal meaning. [2]

List of SHE is as follows [4]:

Rutherfordium	104	Meitnenium	109	Ununquadium	114
Dubnium	105	Dremstedium	110	Ununpentium	115
Seaborgium	106	Roentgenium	111	Ununhexium	116
Bohrium	107	Ununbium	112	Ununseptium	117
Hassium	108	Ununtrium	113	Ununoctium	118

These shell structures for SHEs can be understand in terms of “Magic numbers”, and “island of stability”

1.1 **Magic numbers**: As in an atom the electrons are revolving in the quantized shells similarly in nucleus, the nucleons also form close shells at magic no.’s in 2, 8, 20, 28, 50, 82[5] .From the calculation of the binding energies, we predict that at magic no.’s the stability of the nuclei is relatively higher than other possible combinations of N and Z. We know that every system in the universe tends to go towards stability. So the elements which are higher than Lead (Pb) always

prefer to decays to lead after their formation. As $^{208}Pb_{82}$ is doubly magic so the maximum stability is achieved while decaying into this nucleus. [7]

Similarly, the next higher stability is observed at Z=126, but Z=114 and 120 are giving a tough competition to the Z=126, magicity. In other words the proton shell closures are predicted for Z=114,120,126 by different groups working in super heavy region. On contrary N=184 seems relatively established as next probable neutron magic number after N=126.

As we know that the shell closures are at magic numbers for very stable nuclei's and these magic nuclei's are associated with the Island of stability .Before we go further, we must know about the island of stability and contribution of SHE to this interesting phase space. [2]

1.2 The Island of stability is a term from the nuclear physics that described the possibility of elements with particular stable magic no.'s of protons and neutrons. This would allow certain isotopes to be far more stable than other. The idea of island of stability was first proposed by Glenn I Seaborg [8]. The hypothesis is that the atomic nucleus is built up in shell in a manner similar to electrons shells in atoms. In both the cases shells are just group of quantum energy levels that are relatively close to each other. Energy levels from quantum states in two different shells will be separated by a relatively large energy gap. So, when the number of neutrons and protons completely fill the energy levels of the given shell in the nucleus, the binding energy per nucleon will reach a local maximum and thus that particular configuration will have larger lifetime than nearby isotopes that do have filled shells [3], which can be explained by shell model.

According to shell model, these magic numbers are obtained due to spin-orbit interaction. Due to the spin-orbit interaction the energies of states of the same level are same but with different *j* will no longer be identical [9]. This is because in the original quantum numbers, when $\vec{s}$ is parallel to$\vec{l}$, the interaction energy is negative; and in this case $j = l + s = l + 1/2$. When $\vec{s}$ is anti-parallel to $\vec{l}$ (i.e. aligned oppositely), the interaction energy is positive, and in this case $j = l - s = l - ½$. [9]

Like due to spin orbit interaction, for n=0, L must be 0 and s=1/2 therefore J=0+1/2=1/2 and number of states are determined by the formula: 2J+1(degeneracy), hence 2*1/2+1=2 states are

observed. Similarly for 1p shell n=1, for which l=0, 1 is observed as l varies from 0 to (n-1).Therefore two values of total angular momentum are observed j=1/2,3/2.due to this splitting of levels take place with 2 protons or neutrons in $1p_{1/2}$ and 4 in $1p_{3/2,}$ total 6 states are observed which is shown in figure 3 below:

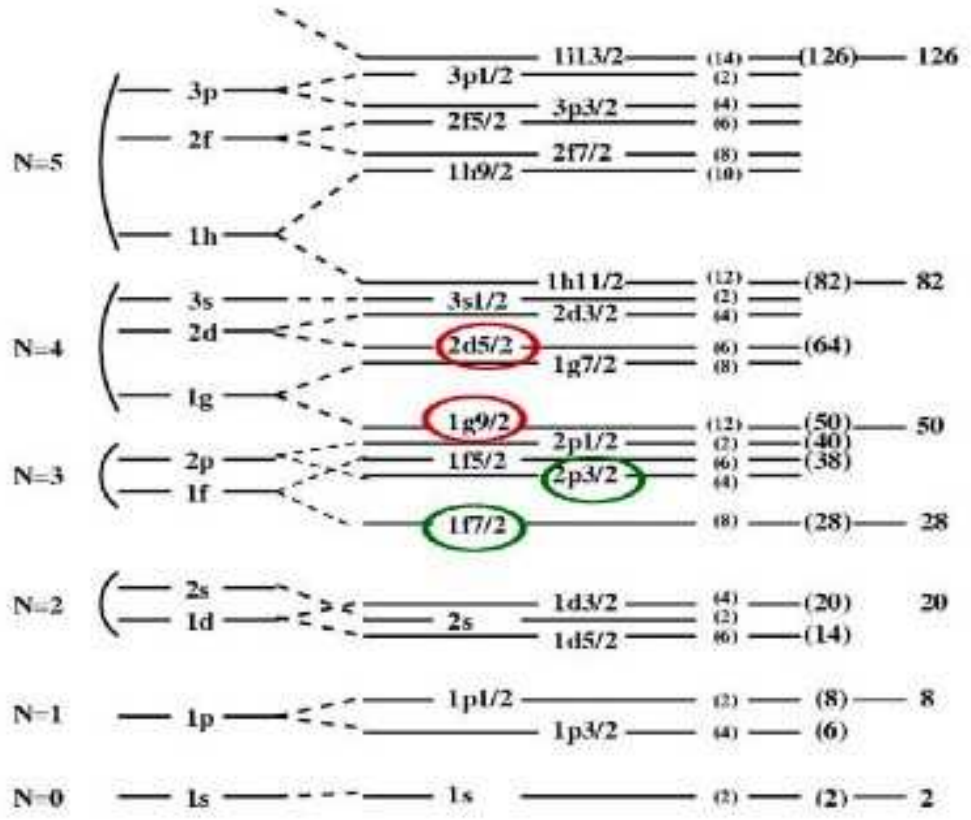

Figure1.3, Nuclear shell closures and Magic numbers. [6]

At these shells following effects [7] are also observed:

1. The neutron absorption cross-sections for isotopes where N = magic number are much lower than surrounding isotopes.
2. The binding energy for the last neutron is a maximum for a magic neutron number and drops sharply for the next neutron added.
3. Electric quadrupole moments are near zero for magic number nuclei.

4. The excitation energy from the ground nuclear state to the first excited state is greater for closed shells.

As we have mentioned earlier, possible magic no. for neutron is 184 and magic protons no.'s are either of 114, 120, and 126. In the island of stability, between bismuth and thorium, there is a severe instability, which renders such elements as radon and francium. But now this sea of instability has drained off and sandbanks, rocky footpaths paved with cobblestones of shell stabilized deformed nuclei are connecting the region of shell stabilized deformed nuclei around Z=114. So 114 is called stepping stone for island of stability [2] but the current investigation for super heavy island reveals that the centre of magic island is Z =110, N=180 appears in the nearest neighborhood and for SHE Z> 116, N=184.

Similarly, according to microscopic-macroscopic model Shell – correction energy is plotted in fig. 1.5[2] .Two equally deep minima are obtained, one at Z=108 and N=162 for deformed nuclei and other one is at Z=114 and N=184 for spherical SHEs .Different results are obtained from self consistent Hartree – Fock –Bogoliubov, HFB, calculations and the relativistic mean field models.[2] They predicted for spherical nuclei shells at Z=114, 120 and 126 (dashed lines in fig.) and N= 182 or 172.

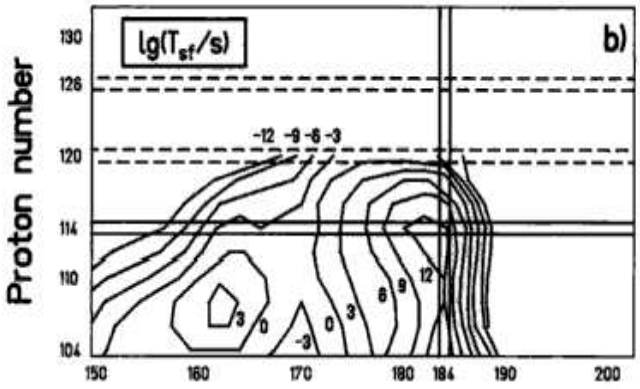

Figure 1.4, Shell – correction energy taken from [2]

Shell stabilizations in SHEs can be understood not only in terms of spin orbit interaction but some other effects are equally important, some of which are discussed later in this chapter.

1.3 Relativistic effects [2]

(1) With increasing Z of heavy or super heavy elements the electrons in the core shell get influenced and as a result ,electron movement become faster with v/c causing a strong attraction to the core of electron which is moving faster with v/c≅0.8.Consequently mass of electron gets modified to

$$m = m_0/[1-(v/c)^2]^{1/2}$$

Where m_0 is a rest mass and v is the velocity of the electron. The effective Bohr radius

$$a_B = \frac{\hbar^2}{mc^2} = a_B{}^0\sqrt{1-(v/c)^2}$$

decreases, as a consequence, for a hydrogen like s and $p_{1/2}$ electrons (the 1s electron of Sg has v/c = 106/137 =.77 so that its radius shrinkage is 37%). The contraction and the stabilization for hydrogen like s and $p_{1/2}$ orbital's is known to be direct relativistic effect and it was shown to originate from inner K and L shell regions. This effect was originally thought to be large only for "fast" electrons in inner core shells of heavy and super heavy atoms. It was, however shown the direct relativistic stabilization is still large for outer s and $p_{1/2}$ orbital's .Example 7s orbital of 105, Dubnium shown in fig 1.6, is $\Delta_R <r>_{7s}$ =25% reletivistically contracted .The contraction of outer s and $p_{1/2}$ orbital's was recently explained as due to admixing of higher bound and (partially) continuum orbital's due to relativistic perturbations [34]

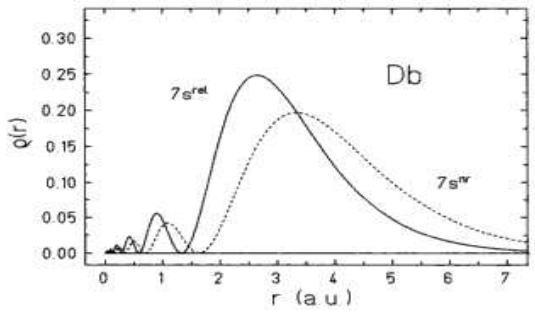

Figure 1.5, Relativistic (solid line) and non relativistic (dashed lines) radial distribution of 7s valance electron in element 105, Db.

The effect of ns orbital contraction reaches maximum in 6th row Au (17.3%) and in 7th row on element 112(31%). The phenomenon is being called relativistic effects gold maximum and group 112 maximum respectively.

ii) The second relativistic effect is expansion of outer d and f orbital's. The relativistic contraction of s and $p_{1/2}$ results in more efficient screening of nuclear charge so that the outer orbital's which never come towards the core becomes more expanded and energetically destabilized .While the direct relativistic effects originates in the immediate vicinity of nucleus , the indirect relativistic effect is influenced by the outer core orbital's. It should be realized that though s and $p_{1/2}$(inner half) core orbital's cause indirect destabilization of outer orbital's , reletivistically expanded d and f orbital's cause the indirect stabilization of the valence s and p orbital's. That partially explain the very large relativistic stabilization of 6s and 7s orbital's of element 112 respectively.

Since d shells (also valid for f shells) becomes fully populated at the end of series, there will occur a maximum of indirect stabilization of valence s and p orbital's [34].Fig.1.7 demonstrates the relativistic stabilization of ns orbital's as well as destabilization of (n-1)d orbital's for group 8 elements as an example . One can see that relativistic and non- relativistic energies of valence electrons are opposite from 5d to 6d elements. Thus , the non- relativistic description of the wave function would still give the right trend in properties from 4d to 5d elements ,while it would result in opposite and consequently wrong trend from 5d to 6d elements .

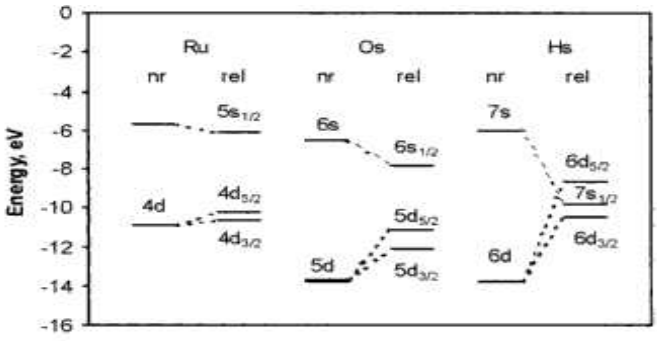

Figure 1.6 .Relativistic and non relativistic energy levels of valance ns and (n-1) d electrons for group 8 elements. [2]

(iii)The third relativistic effect is spin- orbit splitting of the levels with l > 0 (p, d, f…..electrons) into j= +_1/2 .It also originates from the inner region in the vicinity of the nucleus. The spin orbit splitting for the same l decreases with increasing the number of sub shells i.e. it is much stronger for inner cores shells than for outer shells. The spin orbit splitting decreases with increasing l for the same principle quantum number i.e. $np_{1/2}$ –$np_{3/2}$ splitting is larger than $nd_{3/2}$-$nd_{5/2}$ and both are larger than $nf_{5/2}$-$nf_{7/2}$ .It is explained by orbital's densities in the vicinity of nucleus decreases with increasing l .In the transactinide compound spin orbit coupling becomes similar even larger in size as compared to typical bond energies .The spin orbit splitting of the valence 7p electrons in the 118 , example is as large as 11.8eV, see Fig. 1.8

All these relativistic effects are of same order of magnitude and they grow roughly as $Z^{2.}$

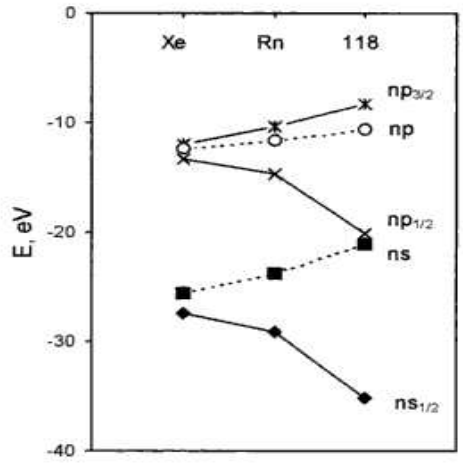

Figure 1.7, Relativistic stabilization of ns and $np^{1/2}$ orbital and spin orbit splitting of np orbital's for noble gases Xe, Rn and element 118.[2]

The exploration of new regions of the nuclear chart is expected to reveal nuclei with unusual sizes, shapes and new decay modes. There is widespread interest in p, 2p, α and heavy cluster emission near proton dip line and both prompt and delayed β.As nuclei move further from β stability on proton side, their binding rapidly decreases, due to increase in columbic repulsion and reaction Q-values which leads to two major difficulties in their studies [10].

(1) One is related to reaction mechanism for their production.

(2) Nuclear decay properties.

The relatively larger Q-values cause high excitation in nuclear systems involved and open up many competing reaction channels favoring the nuclei closer to stability [10] which is explained below.

1.4 Stability of super heavy elements:

Stability of SHE can understand on the basis of three decay modes:

a) Spontaneous fission.

b) α- decay.

c) Cluster decay.

In the case of super heavy elements spontaneous fission and alpha decay are the main decay modes. Theoretically, alpha decay and spontaneous fission share the same underlying mechanism in Physics, i.e. the quantum tunneling effect. The alpha decay process is considered as an alpha cluster penetrating the Coulomb barrier after its formation in the parent nucleus.

As compared to alpha decay, the situation of spontaneous fission is much more complex and there are large uncertainties existing in the fission process such as mass and charge numbers of the two fragments, the number of emitted neutrons and released energy etc.

But new nuclides of super heavy elements from 114 to 120 above preferred to go through sequential α- decay which ends with spontaneous fission. For example 118 undergoes three sequential α- decay followed by spontaneous emission as shown in fig.1.9

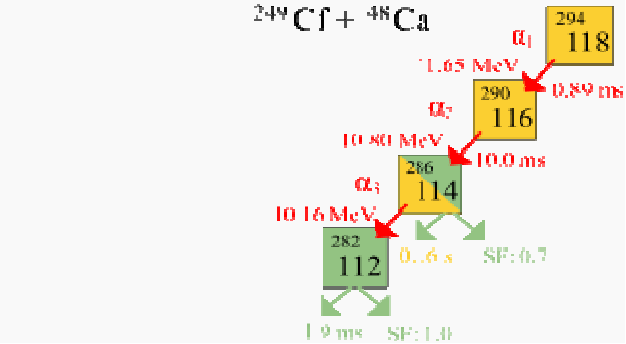

Figure 1.8, 118 undergoes three sequential α- decay followed by spontaneous emission.

Let us understand difference between spontaneous fission and α- decay and cluster decay for SHEs.

1.41 Spontaneous fission is a form of radioactive decay characteristic of very heavy isotopes. It is theoretically possible for any atomic nucleus whose mass is greater than or equal to 100 atomic mass units (u). In practice, however, spontaneous fission is only energetically feasible for atomic masses above 230 u .The elements most susceptible to spontaneous fission are the high-atomic-number Actinide elements, such as mendelevium and lawrencium, and the trans-actinide elements, such as Rutherfordium [4]. Acc. to LDM, spontaneous fission must be most prominent phenomenon in SHE because their half life periods are very small due to excess of neutrons but an amazing fact is observed: Enormous stabilization against fission is gained at these shell closures. But this was the sharp contrast to liquid drop model which predicts the same region for vanishing barriers at shell stabilization and hence prompts disruption [11]. It is well known that the stability of heavy and super heavy nuclei is not governed only by liquid-drop predictions, which suggest that nuclei with $Z > 102$ will spontaneously fission and cannot exist. Quantum shell effects introduce shell stabilization that can make super heavy nuclei live longer. [12]

However according to macroscopic- macroscopic model the macroscopic component measures the average change in coulomb and nuclear energy and microscopic part is the function of charge in the shell structure of deformed nuclear system. This macroscopic component of fission barriers declines rapidly with increase in atomic number due to coulomb energy increasing (proportional to $Z^2/A^{1/3}$) as compared to surface energy (proportional to $A^{2/3}$).For Z>102, the

simple LDM predicts the barriers of less than 1 MeV, which suggests that fission properties and existence itself of those nuclei mainly depends upon shell effects [12].

Due to shell stabilization effects associated with non uniformities may have finite barrier to spontaneous fission .In order to determine the spontaneous fission half lives for SHE, we must know.

a) Ground state Binding energies [2]

b) Size of spontaneous fission barrier [2]

1.41 (a) Binding energy for super heavy elements:

Binding energy of a nucleus or nuclear mass is one of the most important qualities of nuclear ground properties.

1. It plays a crucial role for the stability of the nucleus on β decay, α decay and spontaneous fission of heavy mass region with $Z \geq 90$. [13]

2. The half life of an unstable nucleus is directly related to the value of its binding energy or to the difference of binding energies of neighboring nuclei. [13]

3. In calculations of in cross-section of the binding energies of unknown nuclei are key input quantities of nuclear model i.e. the very accurate predication on binding energies of unknown super heavy nuclei is important not only for estimating the half life of unknown nuclei but also for estimating the production cross-section of SHE.[13]

The calculation of ground state binding energy provides the basic steps to determine stability of SHE. In macroscopic-macroscopic models of B.E is calculated as a sum of predominating macroscopic part (derived from liquid drop model)and microscopic part (derived from shell model).this way more accurate values for B.E are obtained than in the cases of using only the liquid drop model. The shell correction energies of ground state of nuclei near closed shells are negative which results in further decreased value of negative binding energy from LDM and thus increased stability.

Modification in binding energy

The most successful method for the calculations of binding energies is semi empirical mass formula proposed by Weizsacker and Bethe in middle 1930's. Also, some other methods or models for calculating the B.E are:

a) Binding energy calculation by Swiatecki and Moller. [14]

b) Meyers and Swiatecki calculated B.E. by Thomas Fermi model etc [15]

c) Self consistent mean field calculations successfully reproduce properties of many nuclei etc. [16]

These calculations successfully reproduce the experimental B.E. with root mean square deviations of ΔB=0.67-2.0 .So, we consider these models are very successful for the global behavior of nuclear B.E. of the whole mass range i.e. it is very difficult to find the new model to replace these successful models. It is always desirable to use a refined model to make accurate prediction of nuclear B.E in local mass range. It is strongly hoped that a more refined model of binding energies is used for a very accurate prediction of nuclear binding energies in local unknown mass range. For transuranium i.e. SHE region range the half lives of nuclei are extremely sensitive to their decay energies that are the differences of B.E.s of neighboring nuclei.

For example:

a) Moller pointed that an uncertainty of 1 MeV in α-decay half life ranging from 10^5 to 10^3 times for the heavy element region. [14]

b) According to Swiatecki's formula of spontaneous fission, half life formula of an uncertainty of 1 MeV of binding energy can also lead to uncertainty of half life of spontaneous fission with factor 10^4 or 10^5. [15]

So, a new formula of B.E. with precision 0.1 or 0.2 MeV is useful for studies of S.H.E. This is the motivation for the improvement of B.E of super heavy elements.

The liquid drop formula given by Weizsacker and Bethe is:

$$B[Z.A] = a_v A - a_s A^{2/3} - a_C Z^2 A^{-1/3} - a\ a_a \left[\frac{A}{2} - Z\right]^2 A^{-1} + a_{p\delta} A^{-1/2} \quad [17]$$

First of all, modification was done in the LDM formula proposed by authors of [13]for heavy elements, which is given by:

$$B(Z, A) = a_v A - a_s A^{2/3} - a_c Z^2 A^{-1/3} - a_a \left(\frac{A}{2} - Z\right)^2 A^{-1} + a_p \delta A^{-1/2} + a_6 |A - 252| / A - a_7 |N - 152| / N. \quad [13]$$

The maximum deviation of the B.E in this formula is 0.7 MeV and this happens around Z = 100 and N = 152. This should be shell influence around Z = 100 and N = 152. Consequently the authors of [13] introduced two new terms to simulate the shell effects on B.E. of heavy nuclei. This formula gives improvement between experimental binding energies and calculated B.E. Although the much improvement is reached, the agreement between experimental data and calculated ones is not perfect for some nuclei [13]**.** So further modification will be required.

After detailed analysis, authors of Dong et.al [18] found two more characters of the deviations between experimental and theoretical binding energies.

(a)Odd-even staggering exists in the deviations for many isotopic chains especially for odd Z. [18]

(b)A peak at N-Z = 50 is found when we plot the deviations against the neutron excess N-Z. [18]

Due to peak of the deviations between experimental and theoretical binding energies near N – Z = 50 implies additional B.E. for nuclei near line N – Z – 50 = 0.

B.E. formula is further improved for neutron excess:

$$B[Z.A] = a_V A - a_S A^{2/3} - a_C Z^2 A^{-1/3} - a_a \left[\frac{A}{2} - Z\right]^2 A^{-1} + a_P \delta A^{-1/2} +$$

$$a_6 \left|A-252\right|\left\|A-a_7\right|\left|N-152\right|1N+a_8\left|N-Z-50\right|/A \qquad [18]$$

This modification in binding energy formula is claimed to be successful in heavy/super heavy range of nuclear synthesis and decay.

The knowledge of ground state binding energy however is not sufficient for calculation of partial spontaneous fission half-lives. Here it is necessary to determine the size of the fission barrier over a wide range of deformation.

1.41(b) Size of fission barriers of SHEs

As mentioned earlier, nuclei with $Z > 102$ will spontaneously fission and cannot exist. Quantum shell effects introduce shell stabilization that can make super heavy nuclei live longer [12].

(1)It can be seen that there is increase in the fission barrier heights with increase in proton number i.e. columbic repulsion increases, makes SHE increasingly unstable against fission. From fig. 1.10, it can be concluded that, as the height of coulomb barrier get increased by adding more and more protons then it will become difficult for SHE atom to cross it.

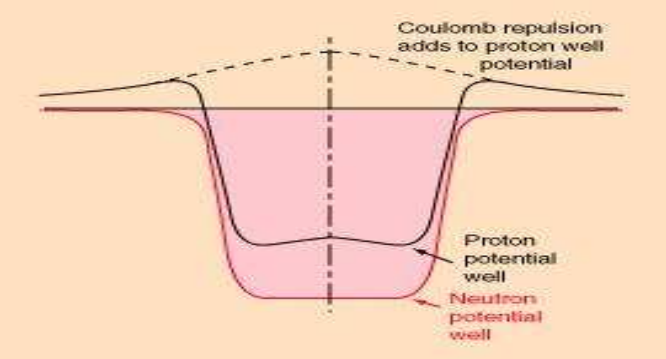

Figure 1.9, Coulomb barrier along with neutron/proton potential well [9].

Also the barrier heights depend upon the neutron numbers along with proton numbers. As neutrons are added beyond 184; the barrier height decreases drastically and when small number of protons are added beyond 114 the barrier height increases [11]. As shown in figure 1.11

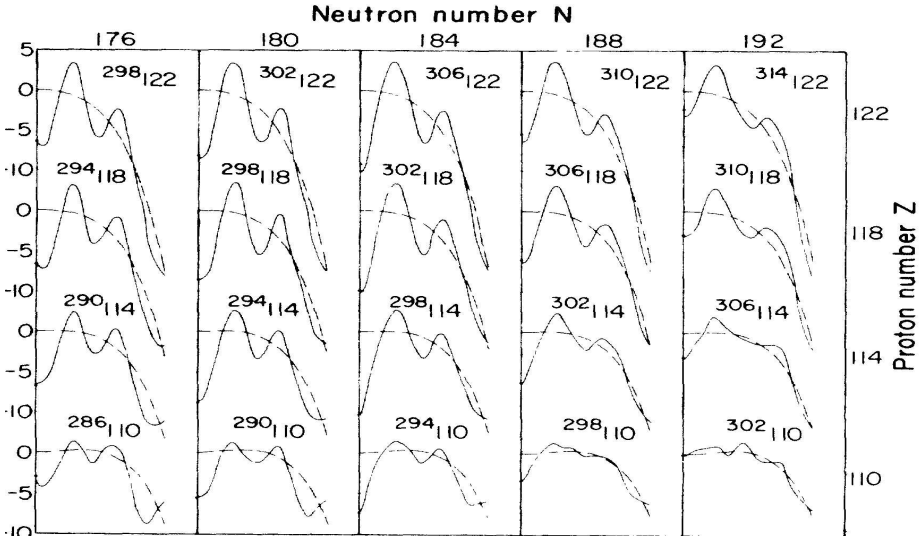

Figure 1.10the dashed curves correspond to LDM and solid lines correspond to shell effects. [11]

(2) The fission barrier depends mainly on the way in which the intrinsic energy of nucleus changes as it slopes varies the intrinsic energy of nucleus undergoes a significant change as its spherically symmetrical configuration turns to deformed configuration.[2]

As these fission barriers and B.E. tells about the stabilities of SHE, two more factors which tell about the stabilities of the SHE, and that is cluster decay and α - decay lives of SHE.

1.42 α- decay half lives:

Alpha decay is a type of radioactive decay in which an atomic nucleus emits an alpha particle, and thereby transforms (or 'decays') into an atom with a mass number 4 less and atomic number 2 less. [19]

Alpha decay is the most common form of cluster decay where parent atom ejects a defined daughter collection of nucleons, leaving another defined product behind (in nuclear fission, a number of different pairs of daughters of approximately equal size are formed). Alpha decay, like other cluster decays, is fundamentally a quantum tunneling process. Unlike beta decay, alpha decay is governed by the interplay between the nuclear force and the electromagnetic force. It typically occurs in the heaviest nuclides, where overall binding

energy per nucleon is no longer a minimum, and the nuclides are therefore unstable toward spontaneous fission-type processes [20].

The reason alpha decay occurs is because the nucleus has too many protons which cause excessive repulsion. In an attempt to reduce the repulsion, a Helium nucleus is emitted. Here is an example of alpha emission with americium-241:

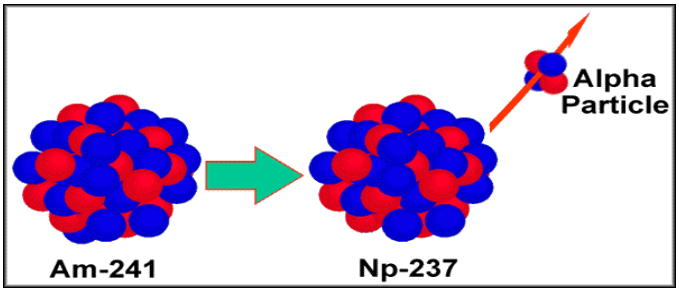

Figure 1.11, Alpha decay from ^{241}Am

And in super heavy elements the quantity of proton is very high hence they are extreme good α-emitters.

Alpha Tunneling Model

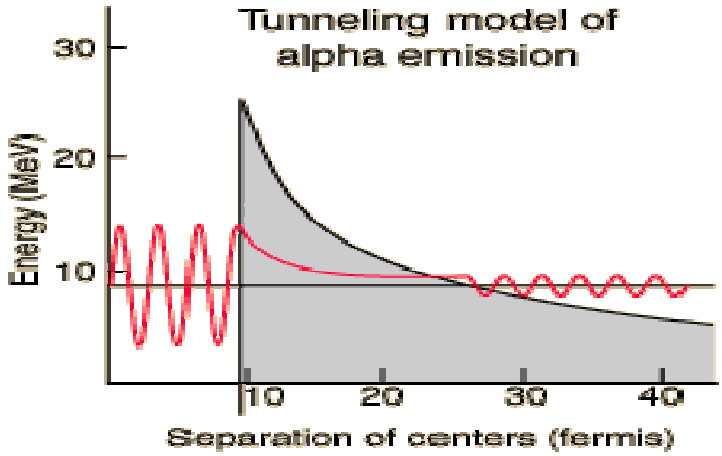

Fig.1.12, Alpha Tunneling Model

Alpha decay is basically a tunneling process. Particle has to cross (tunnel)through it.So, alpha tunneling mainly depends upon the size of the barrier .If the width of barrier is small ,particle

tunnel the barrier easily and if it is not then particle must requires higher energy to pass it. It can be understood as follows [20, 21]:

If a proton is at the edge of a nucleus colliding constantly with walls of nucleus, it can feel the pulling from its neighborhood particles but there is an electromagnetic force, which tends to push it out, all the way from the sides of the nucleus. There is the sensitive balance between these two competing forces. The nucleus need not acquire extra energy to escape; quantum mechanical effect called tunneling allows a certain probability of escape through the wall[g]. But in case of SHEs binding energy is enhanced by several millions eV at shell stabilization, hence, these SHEs mainly at Z=114,120,126 and N=184 or Z=104 have relatively higher α- decay half lives as compared with others SHEs[21]. Hence, the heaviest elements are relatively stable, with half-lives in the region of micro- to milliseconds, and they decay by alpha-emission rather than spontaneous fission. This experimental data proves it that half lives even in seconds and minutes can achieve at these shell stabilizations:

Z	A	$T_{1/2}$
118	294	1.8ms
116	293	53ms
116	291	6.3ms
114	289	2.7ms
112	285	34s
110	279	18s
108	275	15s
106	271	4 min [21]

So, α -emission is the dominant decay mode for SHE with $102 < Z < 120$. Characteristic for these nuclides are very long α -chains as well as parallel sequences of or α-decays terminated by spontaneous fission.

In spite of telling about stability in terms of α-decay, α-decay can also act as the source for providing more information about SHEs.

(1)The long α-half-lives of the nuclei allow the application of the methods of α-spectroscopy, giving new information about nuclear and atomic properties of the heaviest elements. [10]
(2) The study of nuclei passing from spherical to deformed shapes in the course of their consecutive α-decays provides valuable information about the influence of significant structure changes on the nuclear decay properties of SHEs. [10]
(3) Observation and measurements of the typical structures (Clustering and fine structure) in α-decay may provide a powerful method to extend the energy and spin-parity information from daughter to parent with support from theoretical investigations and this may lead to identification of nuclei in long decay chains and determining the excitation energies of the daughter nucleus from decay and in-beam studies. [10]
(4) α-decay chain provides very clear signatures of the nuclides from the beginning of the decay chain, the decay chain can be reconstructed from the bottom, and therefore, it is possible to identify the initial parent through measured α-α (parent-daughter) correlations in the chain.[10]
(5) Also, heaviest known elements were all identified from their α-decay chains, because α-decay chains provide the platform for the production of SHEs in the decay chain whereas fission does not [19], For example:

(i) Ununbium has been observed as decay products of elements 114, 116, and 118. [19]

(ii)Ununtrium has also been detected in the decay of Ununpentium and Ununseptium. [19]

(iii) The isotopes of Ununquadium have also been observed in the decay chain of Ununhexium, Ununoctium and ununseptium which is shown in figure:

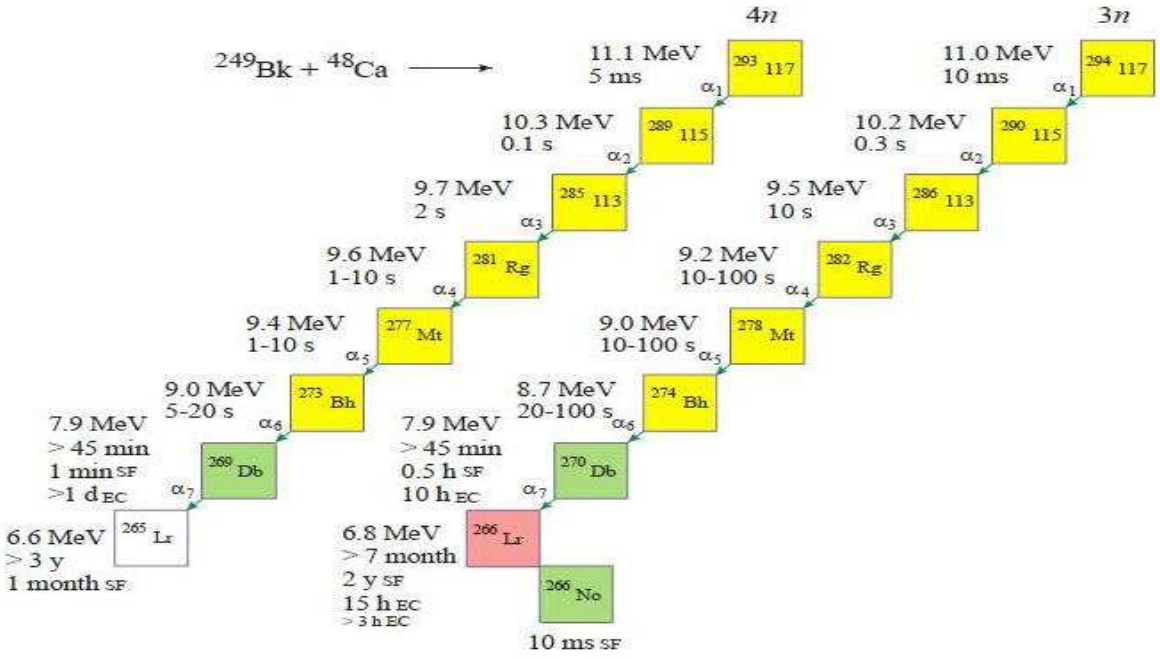

Figure 1.13, Decay chains for 117^{293} and 117^{294} nuclear system.[19]

1.43 Cluster Decay:

The phenomenon of spontaneous emission of particles heavier than alpha particle by radioactive nuclei is known as cluster radioactivity. The rare nature of this process is due to the fact that cluster emission is marked by several alpha emissions [22]. Experimentally, Rose and Jones first observed such decay in 1984 in radioactive decay of ^{223}Ra by emission of ^{14}C.In majority of the cases the possibility of decay is hindered by small barrier penetrability. This quantity reaches large values only in two cases: α-decay and spontaneous fission of heavy nuclei. An exception is given by high penetrabilites of the daughter nuclei^{14} C, ^{24}Ne. This fact is connected too much larger values of ratio of Q_c/B_c relative to the value Q_a/B_a where $B_{c,a}$ are heights of corresponding barriers.[23]

It may be noted that about 15 clusters (mainly isotopes of C, N, O, Ne, F, Mg, Si) have been measured .Majority of these clusters are formed in actinide mass region. In general Q-value of the reaction and shell closures of the daughter nucleus are supposed to be responsible for emission of clusters. However recent studies has shown that the inclusion of deformation and orientation effects is equally important as that of Q-value and shell closure effects in order to make meaningful understanding of cluster radioactivity and related aspects.

Cluster radioactivity is not an isolated phenomenon and must be related to other processes cold fission and cold fusion .This process can be treated as a case of strong asymmetric fission or a decay process of cluster formation and tunneling through the barrier making many assaults on it similar to alpha decay. In cluster radioactivity, the observed daughter nucleus is always a spherical closed- or nearly-closed-shell nucleus. It can be understand more clearly by taking a suitable example of SHEs by considering the cluster decay of $118^{293.}$ [24]

From this fig (1.15) it can be predicted that, the $^{293}118$ decay chain offers two such possibilities: firstly, the ^{14}C decay of the in-between parent $^{281}112$, and secondly, the doubly magic ^{48}Ca decay of any parent nucleus obtained after the α-decay(s) in the investigated chain. The first possibility points out to the deformed magicity of the daughter product $^{267}106$ at $N = 162$ and the second possibility, observation of the doubly magic emitted cluster ^{48}Ca. In the given figure gives good result for heavy cluster decay. [24]

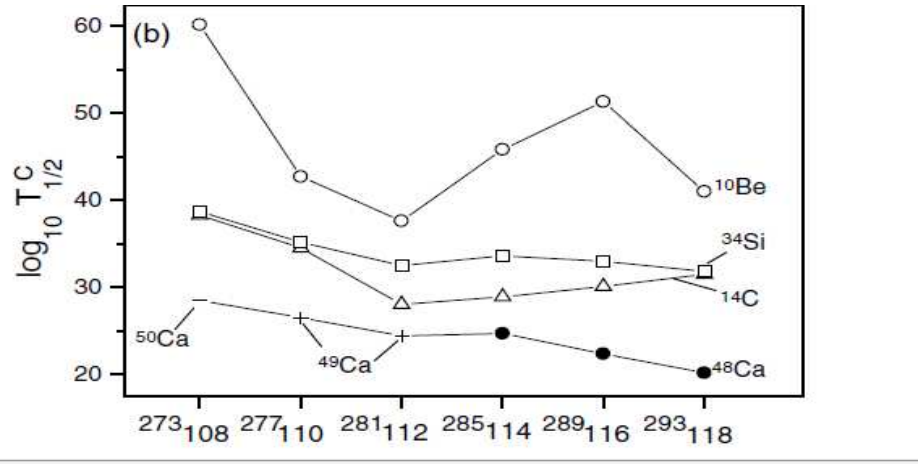

Figure 1.14[24] represents the calculated cluster decay half lives log_{10} T c 1/2 also provides some interesting results:

(i) The shell stabilizing effect, if any, is seen for the ^{10}Be decay of the $^{289}116$ or $^{273}108$ nucleus, since *T c* 1/2 shows strong peaking at these two parent nuclei.

(ii) The ^{14}C decay, in particular from the ^{281}112 parent, seems to present an interesting case of (possibly, a reasonably) deformed magic daughter ^{267}106 with N = 162. This means to say that for the known deformed magic shell at

N = 162 , the ^{267}Sg, not yet synthesized, could also be deformed and observed as the ^{14}C decay of the ^{281}112 parent. From above two points it is clear that in this process, the observed daughter nucleus is always a spherical closed- or nearly-closed-shell nucleus.

(iii) The heavier clusters $^{48–50}$Ca are predicted to decay with further smaller half-lives and hence present themselves as further interesting cases of cluster decay measurements.

Similarlaly some clusters are observed in isotopes ^{294}122 which can be seen from the fragmentation potential graph [22] because the choice of the clusters is always associated with minima in fragmentation potential.

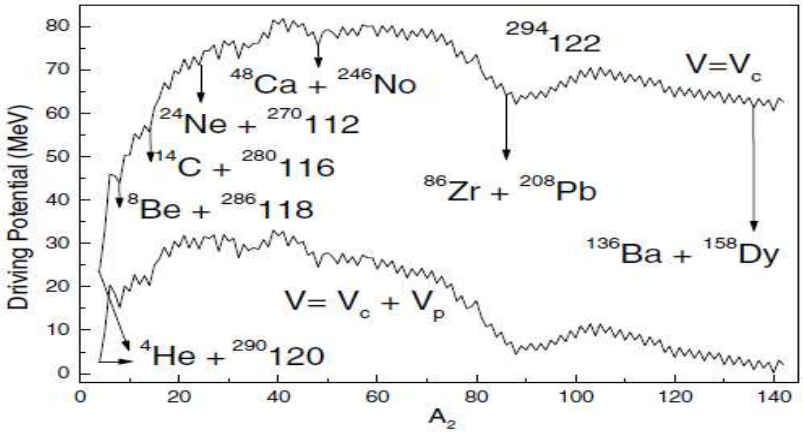

Figure 1.15, Driving potential graph for determining clusters [22] in decay of ^{294}112.

1.5 Synthesis of super heavy elements:

All elements with larger proton numbers have been created artificially in nuclear reactions.

It is known to us those elements with Z>104 exist merely due to these "shell effects". Nuclei where all shells contain the maximum possible number of nucleons ("closed shells") reveal a considerably enhanced stability in comparison to other nuclei, which means that more energy has to be spent in order to excite or decompose them. Hence most appropriate and widely used

method for the synthesis of SHE is fusion evaporation using heavy elements targets, recoil separations techniques and the identification of nuclei by generic ties to known daughter decays after implantation into position sensitive detectors. [2]

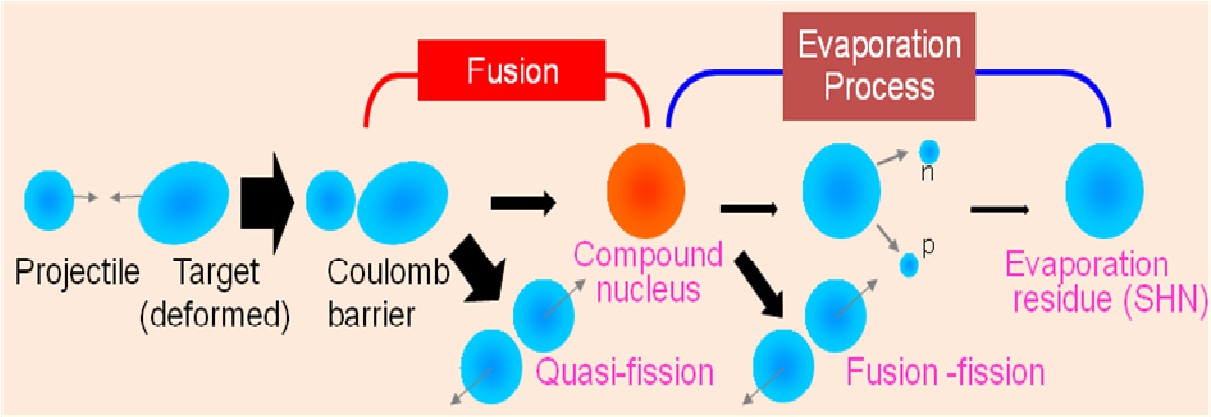

Figure 1.16 represents Fusion and evaporation process for production of SHEs.[25]

So, the main features which determine the fusion process heavy and Supreheavy elements are [2]:

(1) The fusion barrier and the related beam energy and excitation energy.

(2)The ratio of the surface tension versus coulomb repulsion which determines the fusion probability with strongly depends on the asymmetry of the reaction partners.

(3) The impact parameter and related angular momentum.

(4) The ratio of neutron evaporation versus fission of compound nucleus.

In fusion of heavy elements, the product $Z1Z2$ reaches extremely large values and the fission barrier extremely small values. In addition, the fission barrier is fragile at increasing excitation energy and angular momentum, because it is built up solely from shell effects. For these reasons the fusion of heavy elements is hampered, whereas the fusion of lighter elements is advanced through the contracting effect of surface tension. [2]

Hence, two types of fusion are suited for production of heavy and super heavy elements:

(1) Cold fusion

(2) Hot fusion

Synthesis of SHE by hot and cold fusion:

First of all we must understand difference between them. [26]

Cold fusion: Cold fusion reactions use beam and target nuclei that are closer to each other in the mass in order to produce compound nucleus with generally lower excitation energies that typically requires evaporation of one or two neutrons. This generates fewer neutron rich isotopes of an element that have higher probabilities w.r.t fission.

Hot fusion: Hot fusion uses more asymmetric beam and target nuclei produce the compound nucleus with generally high excitation energy that typically requires evaporation of three to five neutrons.

1.51Superheavy elements produced in cold fusion reaction:

In two series of experiments the heaviest elements from 107-109 and from 110 to 112 were synthesis at GSI by using cold fusion.

In cold fusion SHE's are synthesized by of type. X+ (Pb, Bi) =SHE+1n (27)

At near-barrier incident energies, the fusion of heavy nuclei (^{48}Ca, ^{50}Ti, ^{54}Cr, and so on) with ^{208}Pb or ^{209}Bi targets leads to the formation of low-excited super heavy CN (cold synthesis). In spite of this favorable fact (only one or two neutrons are to be evaporated), the yield of evaporation residues sharply decreases with increasing charge of synthesized SH nucleus. There are two reasons for that. First, in these reactions, neutron-deficient SH nuclei are produced far from the closed shells or sub shells. As a result, neutron separation energies of these nuclei are rather high, whereas the fission barriers (macroscopic components plus shell corrections) are rather low. This leads to a low survival probability even for 1*n* and 2*n* evaporation channels. The main reason for low yields of evaporation residues in these reactions is, however, a sharp decrease of the fusion probability with increasing charge of the projectile. [28]

The excitation energy of compound nuclear formed by cold fusion is low 10-20 MeV only and also cross –section for the synthesis of SHE's is very small and deceases strongly with increase atomic number.

Elements (formed by cold fusion) are [26]:

(1)107 Bohrium: was the first new element synthesized using methods of in flight recoil separation. The reaction

$$_{24}Cr^{54} +_{83}Bi^{209} \rightarrow _{107}Bh^{262}$$

(2)108 Hassium: was synthesized in α- decay chains was measured in the irradiation of Pb^{207}, Hs^{269} was discovered as a link in the decay chain of $112^{277,}$ also in this reaction:

$$_{82}Pb^{208} +_{26} Fe^{58} \rightarrow _{108}Hs^{265} + _{0}n^{1}$$

(3)109 Meitnenium: was observed in irradiation of Bi^{209} with Fe^{58} by a single α decay chain

$$_{83}Bi^{209} +_{26}Fe^{58} \rightarrow _{109}Mt^{266} +_{o}n^{1}$$

(4)110 Dremstedium: was discovered using reaction

$$_{28}Ni^{62} + Pb^{208} \rightarrow _{110}Ds^{269} +_{0} n^{1}$$

(5) 111 Roentgenium: investigated using reaction

$$_{83}Bi^{209} + _{28}Ni^{64} \rightarrow _{111}Rg^{272} + _{0}n^{1}$$

(6)112 Ununbium: It was discovered at GSI

$$_{82}Pb^{208} +_{30}Zn^{70} \rightarrow _{112} Uub^{278} \rightarrow _{112}Uub^{277} +_{0}n^{1}$$

1.52 Super heavy Elements Produced by Hot fusion reaction:

Although cold fusion reactions involving a doubly magic spherical ^{208} Pb target and a deformed Projectiles like ^{70} Zn to Produce heavy elements like 110-112, hot fusion evaporation reactions with deformed transuranium target such as ^{224} Pu and doubly magic spherical projectile ^{48} Ca was used for the synthesis of super heavy nuclei Z= 114, 115, 116, 118 at Dubna . Fusion reactions of

^{48} Ca with actinide targets lead to the formation of more neutron-rich SH nuclei than in cold fusion reactions. Unfortunately, weaker binding energies of the actinide nuclei lead to rather high excitation energies of the obtained CN (that is why these reactions are called "hot").[28]
This process was also used to synthesize the elements in mass range 104-108**.**For this mass range cross-section varies for10nb to a few pb with typical beam intensities of $3*10^{12}$ ions per seconds on targets of about 0.8 mg/cm$^{2.}$

Elements produced by hot fusion reaction [26]:

(1) 104 Rutherfordium $_{94}Pu^{242} + _{10}Ne^{22} \rightarrow _{104}Rf^{264}$

(2) 105 Dubnium $^{249}Cf_{98} + ^{15}N_{7} \rightarrow ^{260}Db_{105} + 4_0n^1$

(3) 106 Seaborgium $Cm^{248} + Ne^{22} \rightarrow Sg^{266} + 4_0n^1$

(4) 114 Ununquadium $_{20}Ca^{48} + _{94}Pu^{244} \rightarrow _{114}Uuq^{*292} \rightarrow _{114}Uuq^{289} + 3_0\ n^1$

(5) 115 Ununpentium $_{20}Ca^{48} + _{95}Am^{243} \rightarrow _{115}Uup^{*291} \rightarrow _{115}Uup^{288}$

(6) 116 Ununhexium $_{20}Ca^{48} + _{96}Cm^{249} \rightarrow _{116}Uuh^{293} + 3_on^1$

(7) 118 Uunoctium $_{20}Ca^{48} + _{98}Cf^{249} \rightarrow _{118}Uuo^{294} + 3\ _0n^1$

1.53 Reasons for Hot fusion reactions:

The effect of Coulomb repulsion on the cross-section starts to act severely for fusion reaction beyond fermium. From there continuous decease in cross-section was measured from microbarn for the synthesis of nobelium down to picobarn for the synthesis of 112 .
Actually for Z= 112 measured at GSI, the fusion cross section was extremely small i.e. of 1 pb which led to the conclusion that reaching still heavier elements will be very difficult assignment. We use deformed transuranium targets so that reaction cross section may increase. Their half-lives (elements produce by hot fusion) are several orders of magnitude longer. For example, the half-life of the SH nucleus ^{277}112 synthesized in the cold fusion reaction $^{70}Zn + ^{208}Pb$ [29, 30] is

about 1 ms, whereas $T1/2(^{285}112)$ =34 s [31] (approaching the island of stability). On average, these SH nuclei have higher fission barriers and lower neutron separation energies, which give them a chance to survive in the neutron evaporation cascade.

1.6 Multinuecleon transfer reaction [26]:

The use of multinucleon transfer from a heavy ion projectile to an actinide target nucleus for the production of new nuclear species in the transuranium region has a long history. Light (carbon [32], oxygen and neon [33]), medium (calcium [34, 35], krypton and xenon [36, 37]), and very heavy (^{238}U [38, 39]) projectiles were used, and heavy actinides (up to mendelevium) have been produced in these reactions. The cross sections were found to decrease very rapidly with increasing transferred mass and atomic number of surviving target-like fragments. The level of 0.1μb was reached for chemically separated Md isotopes [39]. These experiments seem to indicate a poor chance for the production of new SH nuclei. However, there is experimental evidence that the nuclear shell structure may strongly influence the nucleon flow in the low-energy damped collisions of heavy ions. For example, in ^{238}U induced reactions on ^{110}Pd at about 6 MeV/u bombarding energy, an enhanced proton flow along the neutron shells $N1$ = 82 and $N2$ = 126 (reached almost simultaneously in target-like and projectile-like fragments) was observed in the distribution of binary reaction products [40].

The idea of taking advantage of the shell effects for the production of SH nuclei in the multinucleon transfer processes of low-energy heavy ion collisions was proposed in Ref. [41]. The shell effects are known to play an important role in the fusion of heavy ions with actinide targets driving the nuclear system to the quasifission channels (into the deep lead and tin valleys) and, thus, decreasing the fusion probability. On the contrary, in the transfer reactions, the same effects may lead to enhanced yield of SH nuclei. It may occur if one of the heavy colliding nuclei, say ^{238}U, gives away nucleons approaching the doubly magic ^{208}Pb nucleus; whereas another one, say ^{248}Cm, accepts these nucleons becoming super heavy in the exit channel—the so-called inverse (antisymmetrizing) quasifission process.

Thus it may conclude that there are several very promising possibilities for the synthesis of new SH elements and isotopes. First of all, use the titanium beam (instead of ^{48}Ca) and actinide targets to move forward up to element 120. The estimated EvR cross sections are rather low (at the level of 0.1 pb) but quite reachable at available setups. If the experiments with a titanium

beam will confirm our expectations, then we have to find a possibility to increase the beam intensity and the detection efficiency (by a total of one order of magnitude) and go on to the chromium and iron beams (aiming at elements 122 and 124). The use of light- and medium-mass neutron-rich radioactive beams may help us explore and fill the "blank spot" at the north-east part of the nuclear map. Such a possibility is also provided by the multinucleon transfer processes in low-energy damped collisions of heavy actinide nuclei, if the shell effects really play an important role in such reactions.

1.7 Uses of super heavy elements [4]:

Despite having numerous features regarding stability or instability of nuclei with in super heavy region, these SHE can be utilized as short lived radioactive species.

As a consequence one may speculate that:

a) They might prove useful as chemical tracers.

b)Some are fantasizing that these SHE may provides the power route necessary for space travel by other life forms with in the universe.

c) An improved understanding of the fission process by studying SHEs will enable scientists to enhance the safety and reliability of the nation's nuclear stockpile and nuclear reactors.

1.8 In the recent era of SHE [4] (recent discoveries in super heavy region)

1. The possibilities of SHE in early moon is reviewed. The siderophic SHE passivity Z= 114, 115, 116 may have been the heat source in the moon's iron core needed to generate the ancient lunar magnetic field. It is suggested that in the search for present day evidence the existence of these hypothetical elements, non meteorites may be a key and scientists are really looking forward with this key.

2. Major research on the observation of long – lived high spin super and hyper deformed isomeric states and the SHE produced in secondary reactions and ordinary heavy ion reactions.

3. Reactions experiments in W targets and prospects for production of SHE in ordinary Heavy seem to give more interesting results.

4. Production of SHE with Z= 112 via secondary and direct Heavy ion reactions are also tried.

5. Discovery of long lived shapes. Isomeric states which decay by strongly retarded high energy particle Radio activity are also being investigated.

6. Coherent Description of Hitherto Unexplained Radioactinites can be understood by super and hyper deformed Isomeric states.

7. Researchers successfully created and detected three new super-heavy isotopes of magnesium and aluminum: magnesium-40, with 12 protons and 28 neutrons; aluminum-42, 13 protons and 29 neutrons; and aluminum-43, 13 protons and 30 neutrons. If the everyday version of aluminum were a 160-pound adult, aluminum-43 would be a muscular, 255-pound heavyweight.

1.9 References

[1]On beyond uranium: journey to the end of the periodic table by Sigurd Hofmann. (Book)

[2] Chemistry of super heavy elements by Matthias Schadel. (Book)

[3]R.Freedman, H.Young (2004), University Physics with Modern Physics, 11th international edition, Sears and Zemansky, 1633-4.

[4] Transactinide elements from Wikipedia.

[5] Nuclear physics by D.C Tayal. (Book).

[6]Nuclear shell model from Wikipedia.

[7]Rohlf, James Williams, Mordern Physics from a to Z0, Wiley, 1994.

[8]Island of stability from Wikipedia.

[9]Cohen, A.B, concepts of Nuclear Physics, Mc.Graw Hill, 1991.

[10] Romanian Reports in Physics, Vol. 57, No. 4, P. 715–746, 2005, Estimates of alpha decay half lives of SHE, W.Scheid and A.O Siliteanu.

[11]Physical review-c, New calculation of fission barriers for haavy and SHE nuclei by M.Bolsesli,E.O Fiest,J.r Nix and J.LNorton.

[12] Physical review C72**,** Role of shapes in the identification of superheavy nuclei, G. Shanmugam, S. Sudhakar, and S. Niranjani, SK Institute of Higher Studies, S-2, Lotus Colony, Nandanam, Chennai - 600 035, India.

[13] Improved version of B.E formula heavy and superheavy elements with Z>=90 and N>=140 by Tiekuang Dong and Zhongzhou Ren, physical review C 72

[14] P.M¨oller, J. R. Nix, and K. L. Kratz, At. Data Nucl. Data Tables 66, 131 (1997)185 (1988).

[15] W. J. Swiatecki's, Phys. Rev. 100, 937 (1955).

[16] P. E. Haustein, special editor, At. Data Nucl. Data Tables 39.

[17] C. F. Von Weizsacker, Z. Phys. 96, 431 (1935), H. A. Bethe and R. F. Bacher, Rev. Mod. Phys. 8, 82 (1936).

[18] T. Dong and Z. Ren, Eur. Phys. J. A 26, 69 (2005).W. Nazarewic, Nucl.Phys.A611, 211(1996).

[19] Alpha decay from Wikipedia.

[20] Physical review C 68, 044316 (2003) α-radioactivity of super heavy nuclei. K. Gambhir, A. Bhagwat, M. Gupta, and Arun K. Jain.

[21] α decay half-lives of new super heavy elements by P. Roy Chowdhury, C. Samanta, and D. N. Basu, Physical review C 73, 014612 (2006).

[22] Alpha decay, cluster decay and spontaneous fission in$^{294–326}$122 isotopes by K P Santhosh and R K Biju, J. Phys. G: Nucl. Part. Phys. 36 (2009) 015107.

[23] Cluster Radioactivity from Wikipedia.

[24]Structure effects in the region of super heavy elements via the α-decay chain of ^{293}118 by Raj K Gupta, Sushil Kumar, Rajesh Kumar1, M Balasubramaniam and W Scheid, J. G: Nucl. Part. Phys. 28 (2002) 2875–2884.

[25] Power point presentation of Nishio by K. Nishio, H. Ikezoe, S. Mitsuoka, I. Nishinaka, H. Makii, Y. Nagame, K. Tsukada ,Japan Atomic Energy Agency, Tokai, Japan.

[26] Elements formed by cold and hot fusion from Wikipedia.

[27] Formation of super heavy elements in cold fusion reactions, Physical review C, volume 63, 044607.

[28]Physical review C 78, 034610 (2008),Synthesis of superheavy nuclei: A search for new production reactions,Valery Zagrebaev and Walter Greiner.

[29] S. Hofmann and G. M¨unzenberg, Rev. Mod. Phys. 72, 733 (2000).

[30] K. Morita *et al.*, J. Phys. Soc. Jpn. 76, No. 4, 043201 (2007); 76, No. 4, 045001 (2007).

[31] Yuri Oganessian, J. Phys. G 34, R165 (2007).

[32] R. L. Hahn, P. F. Dittner, K. S. Toth, and O. L. Keller, Phys. Rev. C 10, 1889 (1974).

[33] D. Lee, H. von Gunten, B. Jacak, M. Nurmia, Y. F. Liu, C. Luo, G. T. Seaborg, and D. C. Hoffman, Phys. Rev. C 25, 286 (1982).

[34] E. K. Hulet, R. W. Lougheed, J. F. Wild, J. H. Landrum, P. C. Stevenson, A. Ghiorso, J. M. Nitschke, R. J. Otto, D. J. Morrissey, P. A. Baisden, B. F. Gavin, D. Lee, R. J. Silva, M. M. Fowler, and G. T. Seaborg, Phys. Rev. Lett. 39, 385 (1977).

[35] A. T¨urler, H. R. von Gunten, J. D. Leyba, D. C. Hoffman, D. M. Lee, K. E. Gregorich, D. A. Bennett, R. M. Chasteler, C. M. Gannett, H. L. Hall, R. A. Henderson, and M. J. Nurmia, Phys. Rev. C 46, 1364 (1992).

[36] K. J. Moody, D. Lee, R. B. Welch, K. E. Gregorich, G. T. Seaborg, R. W. Lougheed, and E. K. Hulet, Phys. Rev. C 33, 1315 (1986).

[37] R. B. Welch, K. J. Moody, K. E. Gregorich, D. Lee, and G. T. Seaborg, Phys. Rev. C 35, 204 (1987).

[38] M. Sch¨adel, J. V. Kratz, H. Ahrens, W. Br¨uchle, G. Franz, H. G¨aggeler, I. Warnecke, G. Wirth, G. Herrmann, N. Trautmann, and M. Weis, Phys. Rev. Lett. 41, 469 (1978).

[39] M. Sch¨adel. Br¨uchle, H. G¨aggeler, J. V. Kratz, K. S¨ummerer, G.Wirth, G. Herrmann, R. Stakemann, G. Tittel, N. Trautmann, J. M. Nitschke, E. K. Hulet, R. W. Lougheed, R. L. Hahn, and R. L. Ferguson, Phys. Rev. Lett. 48, 852 (1982).

[40] W. Mayer, G. Beier, J. Friese, W. Henning, P. Kienle, H. J. K¨orner, W. A. Mayer, L. M¨uller, G. Rosner, and W. Wagner, Phys. Lett. B152, 162 (1985).

[41] V. I. Zagrebaev, Yu. Ts. Oganessian, M. G. Itkis, and W. Greiner, Phys. Rev. C 73, 031602(R) (2006).

CHAPTER-2 METHODOLGY

Introduction

A comprehensive study of various types of emission from the ground state as well as excited states of compound nucleus (CN) formed in low energy reaction is important, as it gives information about the nuclear structure aside the underlying nuclear forces .At low energies and average nuclear force field acts between decaying fragments which in turns ensure possibility of more than one decay path .This average nuclear force field is largely influenced by entrance channel, angular moment and the temperature consideration along with contribution of deformed and orientation effects.

2.1 Features of DCM

(1)The main aim of the work is to study heavy ion reaction dynamics especially the decay of excited compound nucleus using the dynamical cluster decay model (DCM). [1]- [9].

(2) Deformation and orientation effects of the reaction partner and decay products are explicitly included along with temperature and angular momentum contribution in this model.

(3) The ground state cluster decay of radioactive nuclei have also been undertaken with in the preformed cluster decay model [10]-[18].Again having deformation and orientation effects of the cluster as well as daughter nuclei included in it.

(4)DCM (dynamical cluster decay model) and PCM(preformed cluster decay model) works alike ,the only difference is DCM for hot and rotating nuclei (i.e. angular momentum and temperature both not equal to zero) preformed cluster model of Gupta and collaborators for ground state decay (ℓ =0,t=0)in cluster radioactive (CR)and related phenomena.[10]

(5) PCM, DCM is also based upon the dynamical (or quantum mechanical) fragmentation theory of cold phenomena in heavy ion reaction and fission dynamics.

(6)The DCM, worked out in terms of the collective coordinates of mass asymmetry $\eta=\frac{A_1-A_2}{A_1+A_2}$ and relative separation R respectively gives

(a)The nucleon-division (or exchange) between the outgoing fragments

(b) Transfer of kinetic energy of incident channel (E_{cm}) to internal excitation (total excitation or total kinetic energy, TXE or TKE) of the outgoing channel. It may be noted that the fixed decay point R = R_a (defined later),at which the process is calculated depends upon temperature T as well as on η (i.e.(T, η)) .This energy transfer process can be calculated as follows with the help of

E^*_{CN} = $E_{c.m} + Q_{in}$ = IQoutI + TKE (T) + TXE (T) (2.1)

The CN excitation E^*_{CN} is related to temperature T (in MeV) and is given by

$$E^*_{CN} = \frac{1}{9}AT^2 - T(Mev)$$

This model is a two step model

(a) First step is quantum mechanical preformation probability P_0 of the decay products or cluster formed in the mother nuclei

(b)Second step is the penetration of the fragments/ clusters through the interaction barrier.

These two quantities are backbone for calculating cross-section

$$k = \sqrt{\frac{(2\mu Ecm)}{\hbar^2}}; \sigma = \sum_{l=0}^{lg}\sigma l = \frac{\pi}{k^2}\sum_{l=0}^{lg}(2l+1)PoP \quad (2.2)$$

where $\mu = \frac{A1A2}{A1+A2}m$ reduced mass. m is the nucleon mass.

Preformation probability refers to the motion in mass asymmetry coordinate $\eta = \frac{A_1 - A_2}{A_1 + A_2}$;(1and 2 the heavy being heavy and light fragments) and the penetrability P to relative separation R motion. Both preformation probability and the penetrability depend on l and T of the system, and on deformations mass $\beta_{\lambda i}$ and orientations θ_i of the two nuclei or fragments. (λ=2, 3, 4 ,For quadrupole, octupole, hexadecapole deformations)

2.2 How to calculate P_o

The structure information of the CN enters the model via preformation probability P_o (also known as spectroscopic factor) of the fragments given by the solution of stationary Schrödinger equation in η.

$$\left\{-\frac{\hbar^2}{2\sqrt{B_{\eta\eta}}}\frac{\partial}{\partial\eta}\frac{1}{\sqrt{B_{\eta\eta}}}\frac{\partial}{\partial\eta}+V_R(\eta,T)\right\}\psi^{\nu}(\eta)=E^{\nu}\psi^{\nu}(\eta) \quad (2.3)$$

With ν=0, 1, 2, 3….referring to the ground state and excited state solution.

For the decay of the hot compound nucleus, we use the postulate of first turning point

$R_a=R_t+\Delta R\ (T)$ (2.4)

Where $R_t = R_1+R_2$ (2.5)

ΔR(T) is the neck length parameter that assimilates the neck formation effects .This method is introducing a neck length parameter similar to that used in scission point [19] and saddle point [20],[21] statistical fission model. The R_i are radius vectors which are also made temperature dependent can be calculated as

$$R_i(\alpha_i)=R_{0i}\left[1+\sum_{\lambda}\beta_{\lambda i}Y_{\lambda}^{(0)}(\alpha_i)\right] \quad (2.6)$$

with

$R_{0i}(T) = 1.28A_i^{1/3} - 0.76 + 0.8A_i^{-1/3}\times(1 + 0.0007T^2)$, (2.7)

The corresponding potential V (R_a) acts like an efective Q-value, Q_{eff} , for the decay of the hot CN at temperature T, to two exit-channel fragments observed ing.s. (T=0), defined by

$Q_{eff}(T) = B(T) - [B_L(T = 0) + B_H(T = 0)] = TKE(T) = V(R_a(T))$ (2.8)

In terms of $Q_{eff}(T)$, the second turning R_b satisfies (see Fig. 2.1)

$V(R_a, l) = V(R_b, l) = Q_{eff}(T, l) = TKE(T)$. (2.9)

with the l -dependence of R_a defined by : $V(Ra, l) = Q_{eff}(T, l = 0)$, (2.10)

which means that the R_a, given by Eq. (2.4), is the same for all l -values, and that V (Ra, l) acts like an efective Q-value, Q_{eff} (T, l), given by the total kinetic energy TKE(T). Then, using (2.9), R_b (l) is given by the l -dependent scattering potentials, at fixed T as

$$V(R, T, l) = V_c(Z_i, \beta_{\lambda i}, \theta_i, T) + V_p(A_i, \beta_{\lambda i}, \theta_i, T) + V_l(R, A_i, \beta_{\lambda i}, \theta_i, T) \quad (2.11)$$

which is normalized to the exit channel binding energy $B_L(T) + B_H(T)$ Such a potential is illustrated in Fig. 2.1, $_{20}Ca^{48} + _{42}U^{238} \longrightarrow {}_{112}Uub^{286}$ at $\ell = 0$ value. The second turning point R_b is marked for the $l = 0\hbar$ case of $R_a = R_t + \Delta R$ (T). The decay path for the l -values begins at R = R_a.

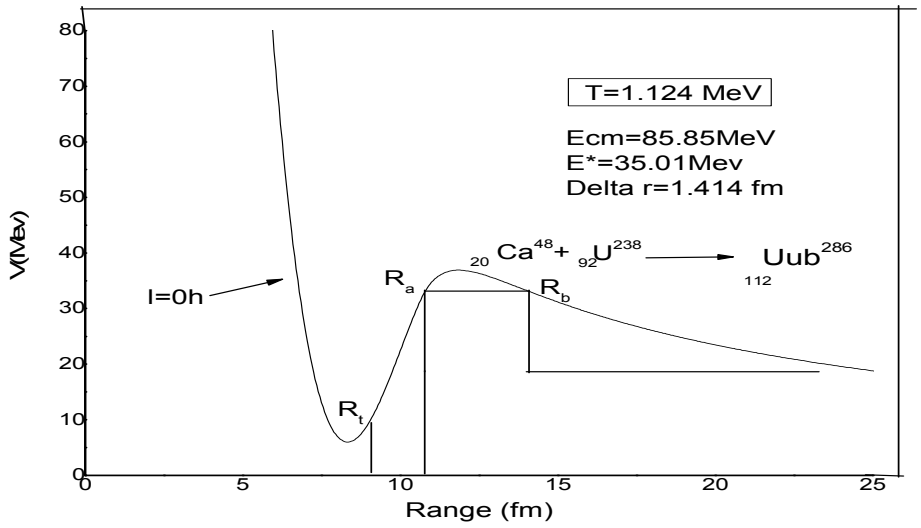

Fig.2.1. Scattering Plot for reaction $_{20}Ca^{48} + _{42}U^{238} \rightarrow {}_{112}Uub^{286}$

The collective fragmentation potential V(R,η,T) in Eq. (2.11) is calculated according to the Strutinsky method by using the T-dependent liquid drop model energy V_{LDM} of [22], with its constants at T=0 re-fitted [3, 4] to give the recent experimental binding energies given by [23], and again refitted [9] to give the recent experimental binding energies[24] and calculate binding energies[25] Then, including the T-dependence also in Coulomb, nuclear proximity, and l -dependent potential in complete sticking limit of moment of inertia, we get

$$V(R,\eta,T) = \sum_{i=1}^{2}[V_{LDM}(A_i,Z_i,T) + \sum_{i=1}^{2}[\delta Ui]exp\left(\frac{-T^2}{T_0^2}\right) + V_c(Z_i,\beta_{\lambda i},\theta_i,T) + V_p(A_i,\beta_{\lambda i},\theta_i,T) + V_l(R,\beta_{\lambda i},\theta_i,T) \quad (2.12)$$

where the T-dependent terms V_c, V_P and V_l are defined as follows: The proximity potential for hot deformed nuclei is [26],[27] (see section 2.3.3)

$$V_p(A_i, \beta_{\lambda i}, \theta i, T) = 4\pi R\,(T)\gamma b(\bar{T})\Phi(s_0(T)) \quad (2.13)$$

and, the Coulomb Potential (see section 2.3.4)

$$V_c\left(Z_i,\beta_{\lambda i},\theta_i,T\right) = \frac{Z_1Z_2e^2}{R(T)} + 3Z_1Z_2e^2 \sum_{i,i=1,2} \frac{R_i^{\lambda}(\alpha_i,T)}{(2\lambda+1)R(T)^{\lambda+1}} Y_\lambda^{(0)}(\theta_i)\left[\beta_{\lambda i} + \beta_{\lambda i}^2 Y_\lambda^{(0)}(\theta_i)\right] \quad (2.14)$$

with the radius vector given by Eq. (2.6) and surface thickness parameter

$$b(T) = 0.99(1 + 0.009T^2) \quad (2.15)$$

The angular momentum potential, (see section 2.3.5)

$$V_l(R,A_i, \beta_{\lambda i}, \theta_i, T) = \frac{\hbar^2\, l\,(l+1)}{2Is(T)} \quad (2.16)$$

with the moment-of-inertia,

$$I_s(T) = \mu R^2 + \frac{2}{5}A_1mR_1^2(\alpha_1, T) + \frac{2}{5}A_2mR_2^2(\alpha_2, T). \quad (2.17)$$

Further, in Eq. (2.12), within the Strutinsky renormalization procedure, we have defined the binding energy B of a nucleus at temperature T as the sum of liquid drop energy $V_{LDM}(T)$ and shell correction $\delta U(T)$ i.e.

$$B(T) = V_{LDM}(T) + \delta U\, exp(\frac{-T^2}{T_0^2}) \quad (2.18)$$

The T dependent liquid drop part of the binding energy $V_{LDM}(T)$ is from Davidson et al. [22], based on the semi-empirical mass formula of Seeger [28]. For the shell correction δU in Eq. (2.17), since there is no microscopic shell model known that gives the shell corrections for light nuclei, we use the empirical formula of Myers and Swiatecki [29].

After modifying the potential used in above stationary Schrödinger equation,

the Schrodinger equation (2.3) can be solved for which the Hamiltonian takes the form:

$$H = \frac{-\hbar^2}{2\sqrt{B_{\eta\eta}}}\frac{\partial}{\partial_\eta}\frac{1}{\sqrt{B_{\eta\eta}}}\frac{\partial}{\partial_\eta} - \frac{\hbar^2}{2\sqrt{B_{RR}}}\frac{\partial}{\partial_R}\frac{1}{\sqrt{B_{RR}}}\frac{\partial}{\partial_R} + V(\eta) + V(R) \quad (2.19)$$

Schrodinger wave equation can be separated for the two co-ordinates η and R as follows,

$$\left[\frac{-\hbar^2}{2\sqrt{B_{\eta\eta}}}\frac{\partial}{\partial_\eta}\frac{1}{\sqrt{B_{\eta\eta}}}\frac{\partial}{\partial_\eta} + V(\eta)\right]\Psi^v(\eta) = E_\eta^v\Psi^v(\eta) \quad (2.20)$$

$$\left[\frac{-\hbar^2}{2\sqrt{B_{RR}}}\frac{\partial}{\partial_R}\frac{1}{\sqrt{B_{RR}}}\frac{\partial}{\partial_R} + V(R)\right]\Psi^v(\mathrm{R}) = E_R^v\Psi^v(\mathrm{R}) \quad (2.21)$$

With $\psi(\eta,R) = \psi(\eta)\psi(R)$

$E = E_\eta + E_R$

The states $\Psi^v(\eta)$ are the vibrational states in the potential V (η) and are labeled by the quantum numbers ν=0, 1,2……

In the following subsections, we first discuss the various the various terms of Schrödinger wave equations (2.20) and (2.21) and then give the solution of eq (2.20) for the determination of preformation probability

$P_0 \propto |\psi^0(\eta)|^2$.

Once the Hamiltonian is established, the Schrödinger equation in mass fragmentation co-ordinate η can be solved. On solving Eq. (2.19) numerically, $|\psi^v(\eta)|^2$ gives the probability P0 of finding the mass fragmentation η at a fixed R on the decay path.

$$P0(A2)=|\psi^v(A2)|^2 \quad (2.22)$$

For fission studies, like the spontaneous fission and fission through the barrier, the motion in R at the saddle point is adiabatically slow as compared to the η motion. Therefore, the potential is minimized in the neck and deformation coordinates ß1 and ß2 at each R and η values. Starting from the nuclear ground state in spontaneous fission or cluster decay, and to have complete adiabaticity, only the lowest vibrational state $\nu = 0$ is occupied. Then, the mass (or charge) distribution yield, proportional to the probability $|\psi^{(0)}(\eta)|^2$ or $|\psi^{(0)}(\eta_z)|^2$ of finding a certain mass (or charge) fragmentation η (or η Z) at a position R on the decay path, when scaled to, say, mass A2 of one of the fragments (d η =2/A) is given by:

$$Y(A_2) = |\psi_R^{(0)}(A_2)|^2 \frac{2}{A}\sqrt{B_{\eta\eta}(A_2)}). \tag{2.23}$$

However, if the system is excited or we allow interaction between various degrees of freedom, higher values of ν would also contribute. These enter via the excitation of higher vibrational states, and through the temperature dependent potential V and masses Bij The effect of adding temperature on potential V and masses B_{ij} is to reduce the shell effects in them, resulting finally in the liquid drop potential V_{LDM} and smoothed (averaged) masses B_{ij} for the systems to be very hot. Apparently, cold fission means taking both the potential V and masses B_{ij} with full shell effects included in them and hot fission means using the VLDM and smoothed (averaged) masses B_{ij}. The possible consequence of such excitations are included here by assuming a Boltzmann like occupation of excited states

$$|\psi(\eta)|^2 = \sum_{\nu=0}^{\infty} |\psi^{\nu}(\eta)|^2 \exp\left(-\frac{E_\eta^\nu}{T}\right) \tag{2.24}$$

Note that we are dealing here with a directly measurable quantity, the mass (or charge) asymmetry, which works dynamically as mass (or charge) transfer coordinate. Thus, the calculated yields Y (Ai) (or Y (Zi)) are directly comparable with experiments. It may be stressed that there is no free parameter in these calculations. The nuclear shape, once minimized in the neck and deformation coordinates ß1 and ß2 at a given R (=Rsaddle), remains fixed for both the mass and charge distributions of fission or decay fragments.

2.3 Overview of potentials used in stationary Schrödinger equation

2.3.1The Scattering Potential V(R)

For a fixed η i.e. for a given outgoing fragment (A_1,A_2) combination, the scattering potential V(R) in Eq. (2.11) is defined as the sum of the deformations, orientations dependent coulomb potential, proximity potential and angular momentum dependent potential, i.e.

$V(R) = V_c(R, Z_i, \beta_{\lambda i}, \theta_i, \Phi) + V_p(R, A_i, \beta_{\lambda i}, \theta_i, \Phi) + V_\ell(R, A_i, \beta_{\lambda i}, \theta_i, \Phi)$ (2.25)

2.3.2 The Fragmentation potential V(η)

The collective potential energy or the fragmentation potential V(η,R), appearing in equation (2.8) is calculated as, V(η,R)=

$$\sum_{i=1}^{2} Bi(Ai, Zi\ \beta\lambda i) + Vc(R, Zi, \beta\lambda i, \theta i, \varphi) + Vp(R, Ai, \beta\lambda i, \theta i, \varphi) + V_l(R, Ai, \beta\lambda i, \theta i, \varphi)$$

The fragmentation potential V (η) is calculated at a fixed distance $R=R_1+R_2+\delta R$ or $R=C_1+C_2+\delta C$ fm, with C_i (i=1, 2) as the sussmann central radii related to the radius vector R_i as $C_i = R_i(1 - b^2/R_i^2)$ with

$$R_i = R_{0i}\left[1+\sum_\lambda \beta\ \lambda i\ Y_\lambda^{(0)}(\alpha i)\right], \quad (2.26)$$

Here λ=2,3,4…. and α_i is an angle that the radius vector R_i of the colliding nuclei makes with the symmetry axis (fig.2.2) the diffuseness of the nuclear surface (I.e. the surface thickness) b = 0.99 fm. The charges Z_i are fixed by minimizing the potential V (η) in the η_Z coordinate at each η value.

For the study of excited systems, where the nuclear temperature effects also come into picture, the fragmentation potential at fixed R is

$$V(\eta, T) = \sum_{i=1}^{2} V_{LDM}(A_i, Z_i, T) + \sum_{i=1}^{2} \delta U \exp(-T^2/T^2_0) + V_c(Z_i, \beta_{\lambda i}, \theta_i, \varphi, T) + V_p(A_i, \beta_{\lambda i}, \theta_i, \varphi, T) + V_l(A_i, \beta_{\lambda i}, \theta_i, \varphi, T) \quad (2.27)$$

Here, V_{LDM} (A_i, Z_i, T) is the liquid drop part of the binding energy and δU, the shell corrections. Note that the calculation of fragmentation potential involves all the possible decay

channels and the number of all such possible decay channels becomes more and more with the increasing mass of the mother nucleus.

2.3.3 The Proximity Potential for deformed, oriented and coplanar nuclei

When two surfaces approach each other within a small distance of less than ~ 2fm, comparable with the surface thickness of interacting nuclei, or when a nucleus is at the verge of dividing into two fragments, then the two surfaces actually face each other across a small gap or crevice. In both cases, the surface energy term alone could not give rise to the strong attraction that is observed when the two surfaces are brought in close proximity. Such additional attractive forces are called proximity forces and the additional potential due to these forces is called the nuclear proximity potential.

Blocki et al. [30] have reanalyzed and extended a theorem, originally due to Deryagin [31], according to which the force between two gently curved surfaces in close proximity is proportional to the interaction potential per unit area between the two flat surfaces. The original expression of Blocki based on the pocket formula was for spherical nuclei, and is given as

$V_P(s_0) = 4\pi\overline{R}\gamma b\Phi(s_0)$. (2.28)

$\Phi(s_0)$ is the universal function, independent of the shapes of nuclei or the geometry of nuclear system, but depends on the minimum separation distance

$$\Phi(s_0) = \begin{cases} -1/2(s_0 - 2.54)^2 - (s_0 - 2.54)^3 \\ -3.437\exp(-s_0/0.75) \end{cases} \quad (2.29)$$

respectively, for $s_0 \leq 1.2511$ and $s_0 \geq 1.2511$. Here, s_0 is defined in units of b, i.e. s_0 is s_0/b. This function is defined for negative (the overlap region), zero (touching configuration) and positive values of s_0. For a fixed R, the minimum distance s_0 for spherical nuclei is defined as

$$s_0 = R - R_1 - R_2$$

where $R = 1.07A_i^{1/3}(i=1,2)$. b is the disuseness of the nuclear surface given by

$$b=[\pi/2\sqrt{3}\ln 9]\, t_{10\text{-}90}$$

where $t_{10\text{-}90}$ is the thickness of the surface in which the density profile changes from 90% to 10%. The value of b ~1 fm. The γ is the specific nuclear surface tension given by

$$\gamma = 0.9517[1\text{-}1.7826(N\text{-}Z/A)^2] \text{ MeV fm}^{-2} \qquad (2.30)$$

R' is the mean curvature radius of the reaction partners, characterizing the gap,

this for spherical nuclei is given by

$$\overline{R} = R_1R_2 / R_1 + R_2$$

2.3.4 The Coulomb potential

Coulomb potential describes the force of repulsion between two interacting nuclei due to their charges. It acts along the line joining the two nuclei. The Coulomb potential for two interacting spherical nuclei is given as

$$V_c = Z_1Z_2e^2/ R$$

For interacting deformed and oriented nuclei, different authors [32]-[36] have derived it differently. In this thesis work, we have started with Coulomb potential of Wong [35], given for two non-overlapping charge distributions, having quadruple deformations only, i.e.,

$$V_c = \frac{Z_1 Z_2 e^2}{R} + \left(\frac{9}{20\pi}\right)^{1/2}\left(\frac{Z_1 Z_2 e^2}{R^3}\right)\sum_{i=1}^{2} R_i^2(\alpha_i)\beta_{2i}P_2(cos\theta_i) + \left(\frac{3}{7\pi}\right)\left(\frac{Z_1 Z_2 e^2}{R^3}\right)\sum_{i=1}^{2} R_i^2(\alpha_i)\left[\beta_{2i}P_2(cos\theta_i)\right]^2 \qquad (2.31)$$

In this expression, the quadrupole-quadrupole interaction term, proportional to $\beta_{21}\beta_{22}$, is neglected since it has a short-range character. For nuclei lying in the same plane we have generalized it to include the higher order deformations (λ = 3, 4...), obtaining

$$V_c(Z_i, \beta_{\lambda i}, \theta_i, T) = \frac{Z_1 Z_2 e^2}{R(T)} + 3Z_1Z_2e^2 \sum_{\lambda, i=1,2} \frac{R_i^{\lambda}(d_i, T)}{(2\lambda+1)R(T)^{\lambda+1}}$$

2.3.5 Rotational Energy due to angular momentum

The rotational motion gives an additional energy due to the angular momentum define as

$$V_l = \frac{\hbar^2 l(l+1)}{8\pi^2 I} \tag{2.32}$$

with $I = \mu R^2$, is the non-sticking limit of moment of inertia with as the $\mu = \frac{A1A2}{A1+A2} m$ reduced mass. m is the nucleon mass. In the complete sticking limit, the moment of inertia I is given as,

$$I = \mu R^2 + 2/5 A_1 m R_1^2 + 2/5 A_2 m R_2^2 \tag{2.33}$$

with R_i from Eq. (2.32). However, for the relative separation of interest here, we use the sticking limit. It is relevant to mention here that value of angular momentum extracted experimentally, is based upon moment of inertia limit. [37]

Another two important terms regarding DCM

2.4 Penetration Probability P

Penetrability P measures the capability of fragments nucleus to penetrate the potential barrier generalized during compound nucleus formation. The penetrability P is the WKB integral between R_a and R_b.

$P=\exp[-2/\hbar \int_{Ra}^{Rb} \{2\mu[V(R)-Q_{eff}]\}^{1/2} dR]$, with R_b as the second turning point , satisfying

$V(R_a, l) = V(R_b, l) = Q_{eff}(T, l_{min}) = TKE(T)$, which means that the potential $V(R_a, l)$, corresponmd to R_a ,acts like an effective Q-value, $Q_{eff}(T, l_{min})$,in the WKB integral, and gives the total kinetic energy TKE(T), where $l_{min}=0$ or refers to the minimum l-value that starts to contribute to WKB integral.

2.5 Assault Frequency υ_0

For the cluster decay studies in the following section, another quantity of interest is the assault frequency υ_0 defined as,

$$\upsilon_0 = \frac{v}{R_0} = \frac{\sqrt{(2E_2/\mu)}}{R_0} \qquad (2.34)$$

where R_0 is the radius of parent nucleus and $E2 = 1/2\mu v^2$ is the kinetic energy of the emitted cluster. Since both the emitted cluster and the daughter nucleus are produced in the ground state, the entire positive Q-value is the total kinetic energy (Q = E1 + E2) available for the decay process, which is shared between two fragments, such that for the emitted cluster

$$E_2 = \left(\frac{A_1}{A}\right)Q \qquad (2.35)$$

And, E1 = Q - E2 is the recoil energy of the daughter nucleus.

2.6 References

[1] R.K. Gupta, M. Balasubraniam, C. Mazzocchi, M. La Commara, and W.Scheid, Phys. Rev. C 65, 024601 (2002).

[2] M.K. Sharma, R.K. Gupta, and W. Scheid, J. Phys. G 26, L45 (2000).

[3] R.K. Gupta, R. Kumar, N.K. Dhiman, M. Balasubraniam, W. Scheid, and C.Beck, Phys. Rev. C 68, 014610 (2003).

[4] M. Balasubraniam, R. Kumar, R.K. Gupta, C. Beck, and W. Scheid, J. Phys.

G 29, 2703 (2003): R.K. Gupta, M.K. Sharma and B. Singh, Phys. Rev. C-tobe published

[5] R.K. Gupta, M. Balasubraniam, R. Kumar, D. Singh, and C. Beck, Nucl.Phys. A 738, 479c (2004).

[6] R.K. Gupta, M. Balasubramaniam, R. Kumar, D. Singh, C. Beck, and W.Greiner, Phys. Rev. C 71, 014601 (2005).

[7] B.B. Singh, M.K. Sharma, R.K. Gupta, and W.Greiner, Int.J. Mod.Phys.E15, 699 (2006)

[8] R.K. Gupta, M. Balasubraniam, R.Kumar, D.Singh, S. K. Arun and W.Greiner, J.Phys .G:Nucl.Part. Phys. 32, 345(2006)

[9] B.B. Singh, M.K. Sharma, R.K. Gupta, Phys.Rev. C 77, 054613 (2008)

[10] R.Gupta, in proceedings of the 5th International Conference on Nuclear Research Mechanics, Varenna, 1988, edited by E. gladioli , (Ricerca Scientifica ed Educazione Permanente ,Milano, 1988),p.416.

[11] S.S. Malik and R.K.Gupta, Phys.Rev.C 39, 1992(1989)

[12] R.K.Gupta, W.Scheid, and W.Greiner, J.Phys.G: Nucl. Part. Phys. 17, 1731(1991).

[13] S. Kumar and R.K.Gupta, Phys.Rev. C 49, 1922(1994).

[14] R.K.Gupta and W. Greiner Int. J. Mod. Phys. E 3, 335 (1994, Suppl.).

[15] S. Kumar and R.K.Gupta, Phys. Rev. C 55, 218 (1997).

[16] R.K. Gupta, in Heavy Elements and Related New Phenomena ,edited by W.Greneir and R.K Gupta (World Scientific Singapore) Vol.II ,p.730

[17] S.K and R.K Gupta, DAE nucl.Phys. (Sambalpur) 52,365(2007)

[18] B.B.Singh, S.K Arun, M.K.Sharma, S.Kanwar and Raj K.Gupta, DAE Nucl.Phys. (Roorkee), Accepted (2008)

[19] T. Matsuse, C. Beck, R. Nouicer, and D. Mahboub, Phys. Rev. C 55, 1380 (1997).

[20] S.J. Sanders, D.G. Kovar, B.B. Back, C. Beck, D.J. Henderson, R.V.F. Janssens, T.F. Wang, and B.D. Wilkins, Phys. Rev. C 40, 2091 (1989t).

[21] S.J. Sanders, Phys. Rev. C 44, 2676 (1991).

[22] N.J. Davidson, S.S. Hsiao, J. Markram, H.G. Miller, and Y. Tzeng, Nucl. Phys. A 570, 61c (1994).

[23] G. Audi and A.H. Wapstra, Nucl. Phys. A 595, 4 (1995).

[24] G. Audi and A.H. Wapstra and C. Thiboult, Nucl. Phys. A 729, 337(2003).

[25] P. M¨oller, J. R. Nix, W. D. Myers, and W. J. Swiatecki, At. Data Nucl. Data Tables 59, 185 (1995).

[26] R.K. Gupta, N.Singh, and M. Manhas, Phys. Rev. C 70, 034608 (2004)

[27] R.K. Gupta ,M.balasubramaniam, R.Kumar, N.Singh, M.Manhas, and W. Greiner, J.Phjs. G: Nucl.Part. Phys. C 31, 631(2005).

[28] P. A.Seeger, Nucl. Phys. 25, 1 (1961)

[29] W. Myers and W.J. Swiatecki, Nucl. Phys. 81, 1 (1966).

[30] J. Blocki, J. Randrup, W. J. Swiatecki, and C. F. Tsang, Ann. Phys. (NY) 105, 427 (1977).

[31] Deryagin, Kolloid Z. 69, 155 (1934).

[32] N. Malhotra and R.K. Gupta, Phys. Rev. C 31, 1179 (1985).

[33] M M¨unchow, D Hahn and W Scheid, Nucl. Phys. A 388, 381 (1982).

[34] M J Rhoades-Brown, V E Oberacker, M Seiwert and W Greiner, Z. Phys. A 310, 287 (1983).

[35] C Y Wong, Phys. Rev. Lett. 31, 766 (1973).

[36] R Aroumougame and R K Gupta, J. Phys. G: 6, L155 (1980).

[37] S.Kailais(private communication)

Chapter -3 Role of deformations in the decay of ^{286}Uub

3.1 Introduction

The decay of ^{286}112 formed in ^{48}Ca+^{238}U reaction has been studied experimentally [1] and the fusion evaporation residue cross-sections have been measured at excitation energies E*∽30-40 MeV. Considering that ^{48}Ca nucleus forms compact configuration with ^{238}U so $\theta_c = 90^o$ is taken and equatorial compact configuration is considered for present set of calculations. The results for non-equatorial configuration $\theta_c < 90^o$ (non-equatorial compact,nec) are shown in recent investigations [2] where the issue related to island of stability for super heavy elements has been addressed by considering three proton magic numbers Z=114,120and126 .As these calculations clearly show that the island of stability for super heavy nuclei centers around Z=126 [3-5] instead of Z=114or Z=120 .So for present set of calculations we have taken Z=126 as proton magic number in order to understand the decay path of super heavy system 112^{286} .It may be important to note that $_{20}Ca^{48} + _{92}U^{238} \longrightarrow _{112}Uub^{286}$ is the hot fusion reaction, here only 3n and 4n emissions are measured.

(1) First of all, we try to fit production cross-section of $_{112}Uub^{286}$ at three different energies [1] E*=31.2 MeV, 35.01 MeV, 39.9 MeV using deformation effects upto hexadecapole in this optimum orientation approach and compare it with experimental data.

(2) Secondly, temperature effect on Fragmentation potential and consequently in Preformation probability, Penetrability is studied at two different temperatures at T=1.124 which is original temperature for E*=35.01MeV and T=1.8MeV (arbitrary high temperature).

(3) We also tried to fit ΔR (neck length parameter) for spherical consideration at same temperature T=1.124MeV at E*= 35.01MeV for same compound nucleus. The DCM comparison could not be worked out with in spherical fragmentation, which clearly means that role of deformations is extremely desirable in order to study the decay of $_{112}Uub^{286}$ nucleus formed in a ^{48}Ca induced reaction.

As it was mentioned in chapter- 1 that fragmentation potential is always associated with choice of clusters (minima in the fragmentation potential).So, these calculations carry useful information regarding the fragmentation process of super heavy nucleus under investigation.

3.2 Results and Discussions:

Fig 3.1 shows the mass fragmentation potential V (A2) for the compound nucleus $_{112}Uub^{286}$ at $R=R_a=R_t+\Delta R$, $\Delta R=1.414fm$ at temp T=1.124MeV corresponding to one of the incident energies Ecm=85.85 MeV, using deformations upto hexadecapole i.e. $\beta_2+\beta_3+\beta_4$ with magic numbers for super heavy region as Z=126, and N=184.

In this figure, for A=122, we see an enhanced minima along with similar dips in this mass region. These minima's clearly show the dominance of these fragments as decay product at least on the basis of potential consideration. However it will be of extreme interest to look out for the penetration probability of these fragments before reaching at final conclusion. The fragmentation potential is depicted as a function of fragmentation mass for extreme values of angular momentum i.e. ℓ =0 and ℓ_{max} where ℓ_{max} is decided at a point where cross-section of light particles become negligibly small. One may clearly see here that at lower ℓ -value the ER are more prominent as compare to fission fragments where as at higher ℓ -values ($\ell=\ell_{max}$) fission fragments start comparing with ER.

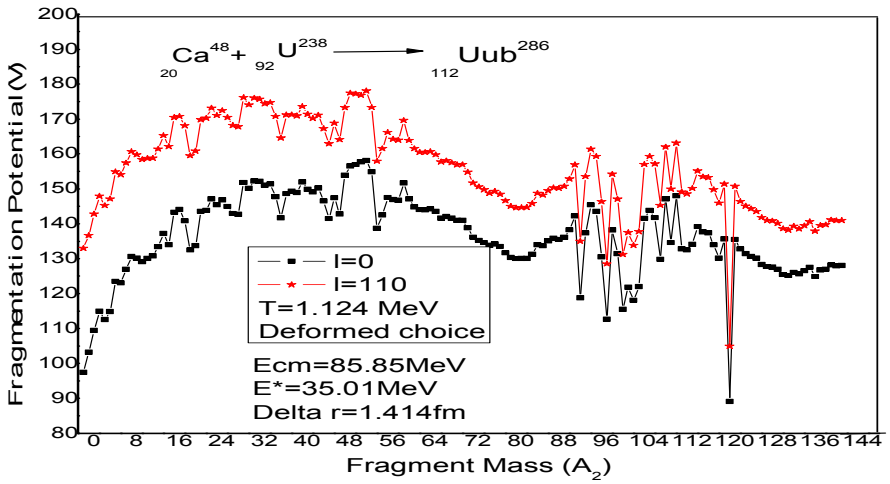

FIG 3.1, Fragmentation potential as a function fragment mass at ℓ =0 and $\ell=\ell_{max}$

Fig.3.2 represents the effect of temperature on the fragmentation potential i.e. how the fragmentation potential varies as temperature changes from T=1.124 MeV and T=1.8MeV, it also reflects the same minima or depths. One may see that the effect of temperature is quite marginal for heavier fragments, however for higher fragments up to A∽50 the fragmentation potential decreases as a function of temperature i.e. probability of formation of lighter fragments gets enhanced with increase in temperature. The neck length parameter is kept same (ΔR=1.414fm) at both temperatures as there is no data as corresponding to higher temperature i.e. T=1.8 MeV.

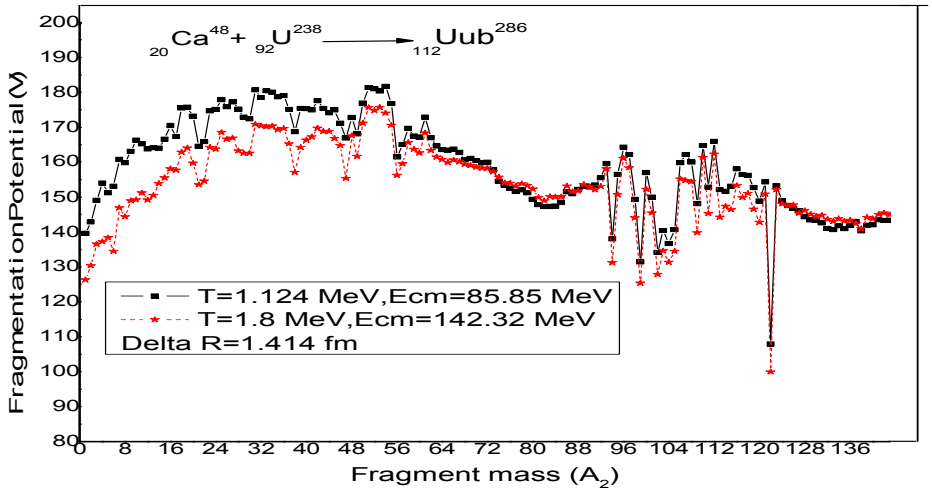

Fig 3.2, Effect of temperature on fragmentation potential as the function of A_2 (Fragment Mass)

Fig3.3, shows the comparison of deformed choice of fragmentation with spherical one at E*=35.01 MeV. One may clearly see that mass fragmentation is relatively smooth with spherical choice (no strong dips are reported) where as there seems to be more structure in fragmentation path with inclusion of deformation and orientation effects. It may be noted that we are not able to fit experimental data in the spherical choice of fragmentation, which simply means that the role of deformations is extremely desirable in order to investigate the decay path of 112^{286} ,However for comparison purpose we have shown the fragmentation path using spherical fragmentation at same neck length value ΔR=1.414fm as that for deformed fragmentation.

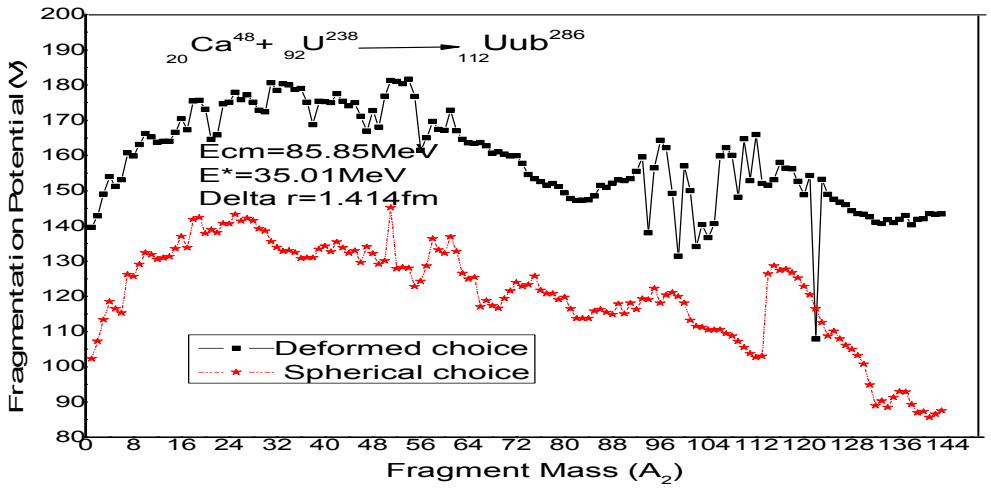

FIG 3.3, Comparison of fragmentation path of deformed with spherical choice at E=35.01 MeV*

Fig .3.4 shows the variation of Preformation probability P_0 as the function of fragment mass number, calculated at ℓ -value $\ell = \ell_{max}$ =110ħ and ΔR=1.414fm at temp T=1.124MeV. Maximum Preformation probability is equal to 0.4944 is seen for fragments mass A=122 and 163. Clearly the mass fragmentation is asymmetric with fairly large contribution of fragments in the vicinity of A_2= 122 and 163.

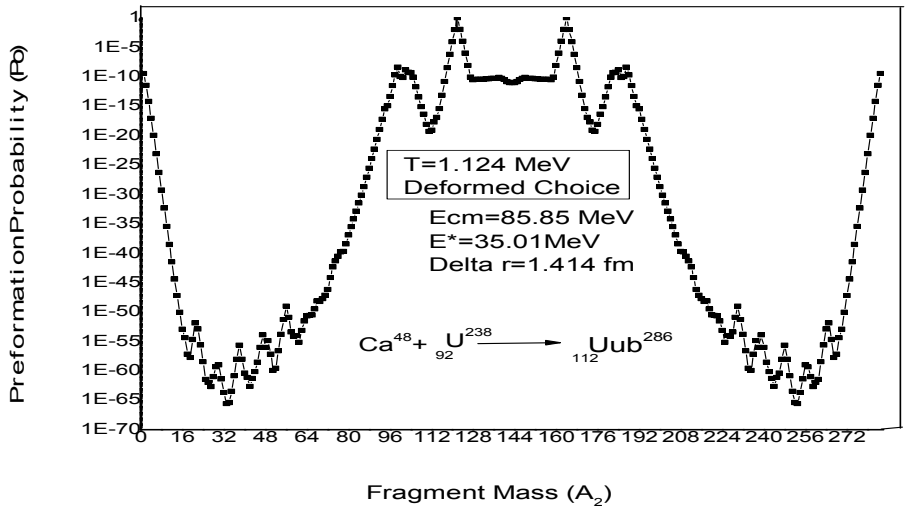

FIG 3.4 shows variation of Preformation probability as the function of Fragment Mass (A_2).

Fig.3.5 represents the effect of temperature by calculating the Preformation probability at temperature other than T=1.124 MeV i.e. at T=1.8 MeV, here the only difference is: at T=1.8MeV, the probability is little bit higher as compared with probability at T=1.124 MeV ,Although the fragmentation path remains largely unaffected with increase in temperature.

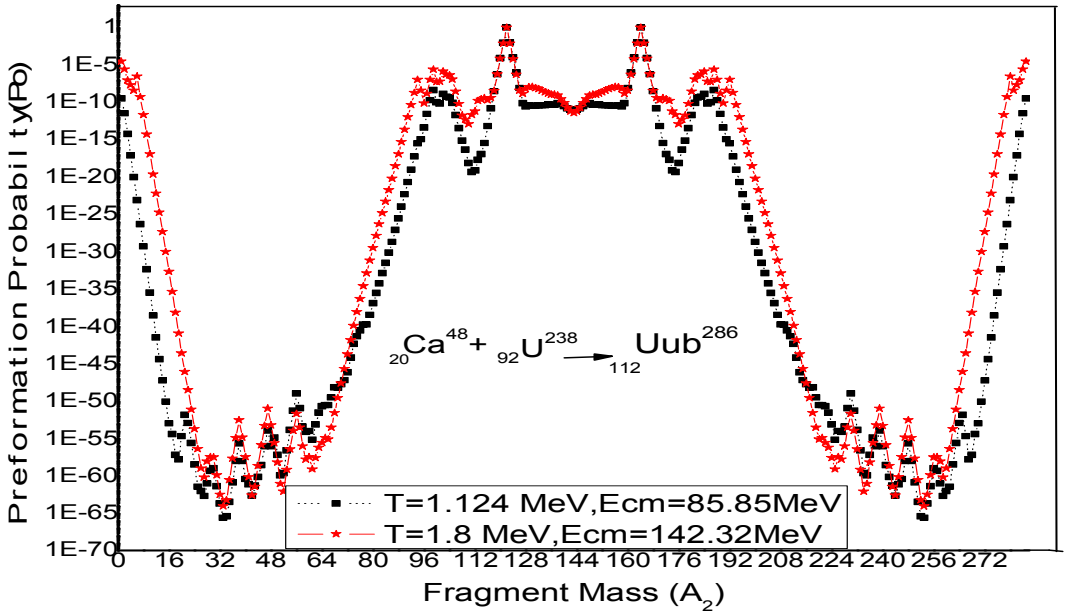

FIG 3.5, Preformation probability at two different temperatures as a function of fragment mass (A_2).

In fig 3.6, we have compared the Preformation probability of 112^{286} super heavy compound nucleus within spherical and deformed choice of fragmentation. One may observe that the mass fragmentation is near symmetric with spherical choice and it becomes asymmetric centering around A2=122 and 163 .This change in fragmentation path with and without deformation effects can be utilized to establish extent of deformations in the decay process of this super heavy nucleus.

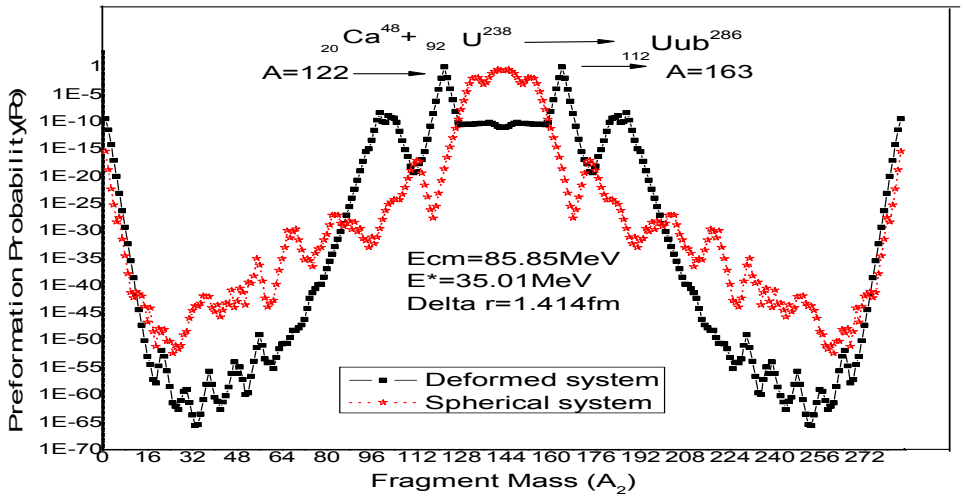

Fig 3.6, Comparative study of Preformation probability as the function of fragment mass with and without inclusion deformation effects.

Another factor that contributes to the cross-sections within DCM approach is, the Penetration probability P, which is shown fig.3.7 .In this graph , the valleys or dips are obtained at fragment masses as obtained in the case of fragmentation potential at A=121,94. Therefore we can say, the prominence of these fragments in fragmentation potential or Preformation probability is counter balanced by their negligibly small penetrability.

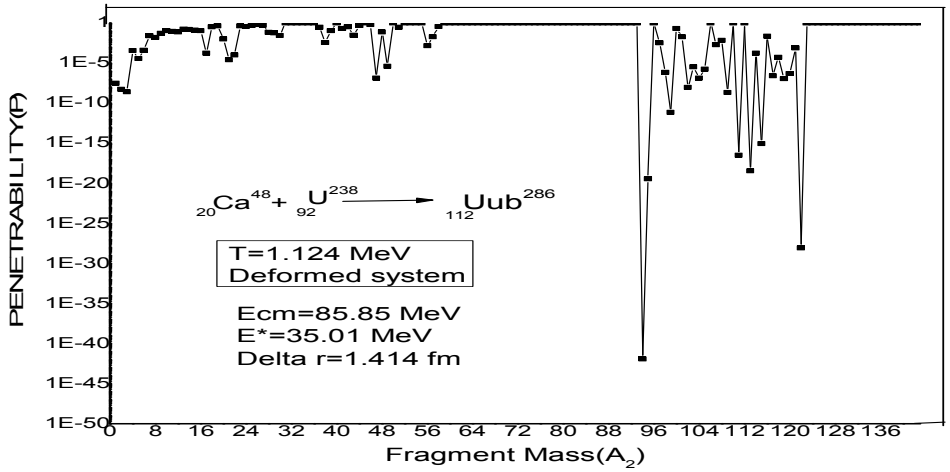

FIG3.7, variation of penetration probability as the function of fragment mass (A2).

In fig.3.8 the effect of temperature is observed on penetrability at T=1.124 MeV and T=1.8 MeV. From this figure it can be clearly seen that the change of temperature affects the penetrability almost negligibly.

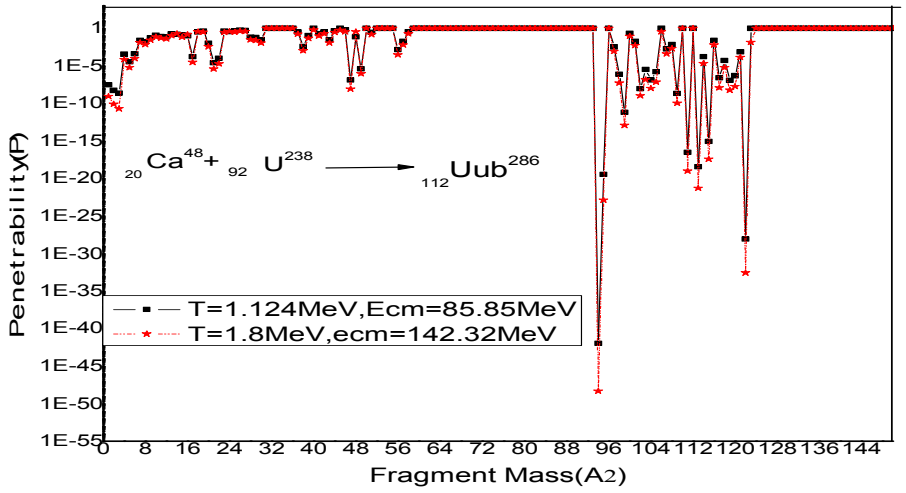

Fig 3.8, Variation of Penetration probability at two different temperatures.

Comparative study (Fig.3.9) of penetrability for spherical and deformed fragmentation tells us that penetration probability show structure with spherical choice where as some interesting variation is seen in mass region 85∽130 with inclusion deformation effects.

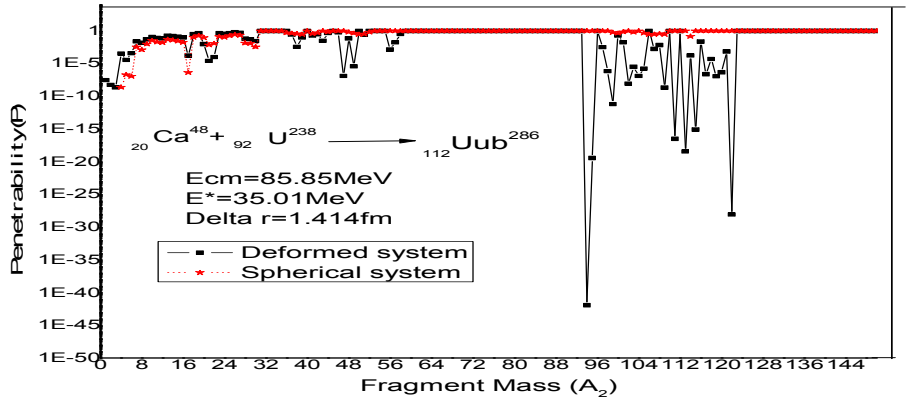

Fig 3.9, Comparative study of penetration probability of spherical and deformed system as a function of fragment mass (A_2).

Experimental values of cross sections are obtained by calculating the cross-section of 3n and 4n channels up to a ℓ_{max} t allowed ΔR i.e. 1.414fm. The ℓ_{max} can be calculated using following procedure.

The channel cross-section in Fig 3.10 obtained at Ecm=85.85Mev and T=1.124 MeV for 3n+4n system, increases with ℓ upto ℓ =53Ћ, but then decreases with further increase in l and finally becomes negligible at ℓ =110 Ћ .As ℓ_{max} is decided at a point where σ_{ER} --→0.So ℓ =110 Ћ is taken as ℓ_{max} for present study .In preset case data is available only for 3n and 4n channel so the ℓ_{max} is decided at a point where σ_{3n+4n}-→0.

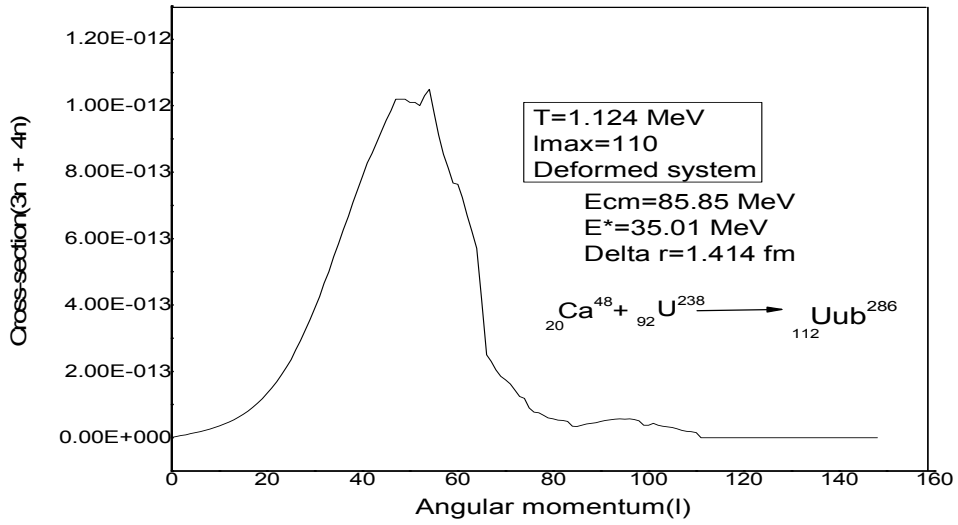

Fig.3.10, Variation of cross-section (3n+4n) as a function of angular momentum.

The Channel cross-section separately plotted for 3n and 4n channel are shown in fig.3.11. For 3n-system channel cross-section increases up to 23Ћ with increase in angular momentum, then decreases with further increase in ℓ and hence ℓ_{max} = 75 Ћ is obtained, similar effects are observed in 4n- system channel cross-section increase upto ℓ=26Ћ with ℓ_{max} =66Ћ.Therefore it is of interest that ℓ_{max} comes out to be different if we take σ (3n+4n) together or σ_{3n} and σ_{4n} individually.

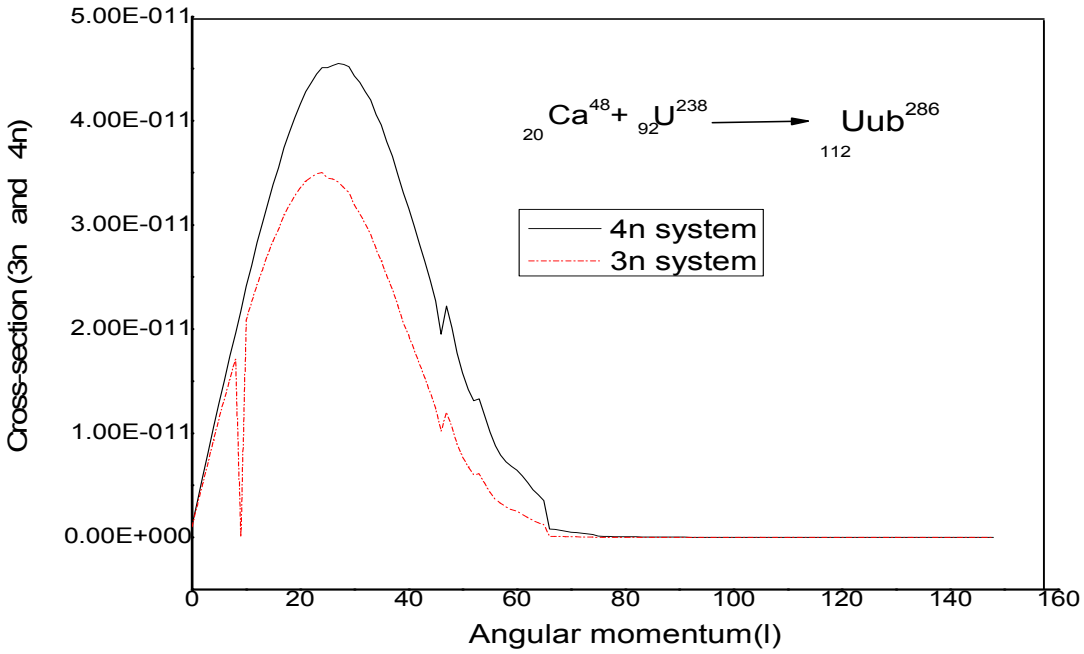

Fig3.11, Variation of individual cross-section for 3n and 4n system as a function of angular momentum.

Finally the DCM calculated cross-sections are plotted in Fig.3.14 which shows negligible deviations with experimental data. The cross-section are plotted at three different energies for 3n+4n system i.e. at E*=31.9 MeV, 35.02 Mev, 39.9 MeV.

Individual cross-sections for 3n and 4n are also plotted in this figure. The near exact comparison of DCM with experimental data shows the importance of remarks made in this work in reference to decay of a super heavy nucleus formed in ^{48}Ca induced reaction.

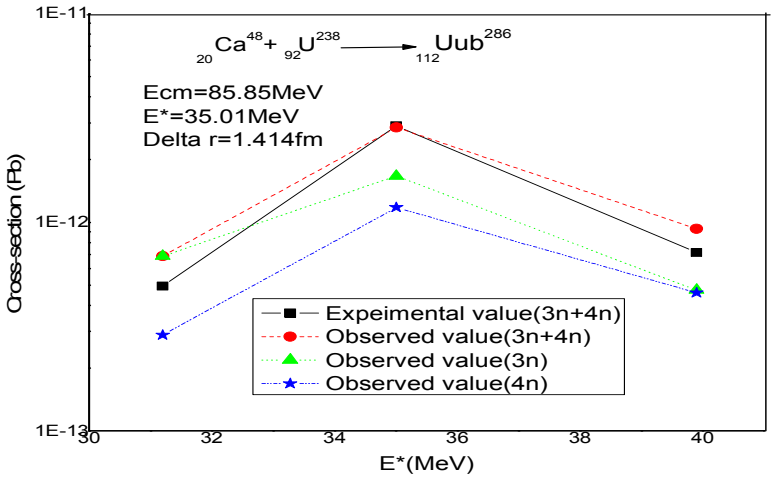

Fig.3.12, Comparison of cross-section σ (3n+4n) with experimental and observed values along with individual cross-sections of 3n and 4n system.

Finally, the summed up cross-section, Preformation probability and penetrability are shown in fig 3.13. Summed up cross-section, Preformation probability and penetrability are plotted upto ℓ_{max} as the function of A_2 (fragment mass number) at Ecm=85.85 MeV, T=1.124 MeV and ΔR=1.414fm.

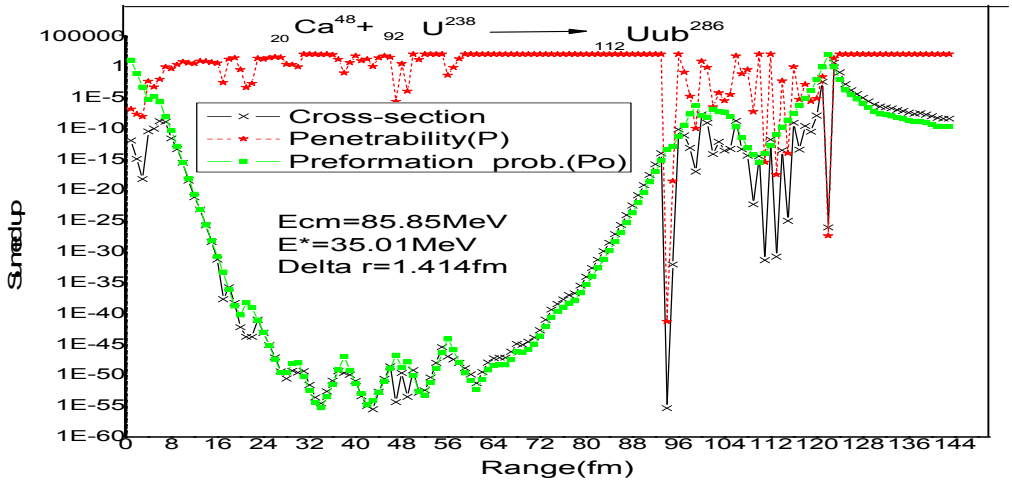

Fig 3.13,Summed up cross-section, P, Po as a function of range (fm).

Clearly Preformation probability seems to have nice structural variation with cross-section. One may see that cross-section and Preformation probability go neck to neck for majority of fragments (except A_2=80∽130) where as penetration probability seem to be contributing only towards magnitude except for reported mass region A_2=85∽130 where it shows interesting structure . Therefore one may note that the fragment masses in mass range A_2=85∽130 need to be investigated further with non equatorial configuration i.e. θ_c <90^o before reaching at final conclusion.

It may be reminded here that present set of calculation is done by presuming proton magicity as Z=126 instead of Z=114 and Z=120 as predicted by [2-5]. It is relevant to mention that DCM has been applied quite extremely in light, medium and heavy mass region however very limiting application are done so far in super heavy region.

It will be of further interest to see the role of modified binding energies [6] discussed in chapter 1 (using modified expression binding energy):

$$B[Z.A]=a_V A-a_S A^{2/3}-a_C Z^2 A^{-1/3}-a_a\left[\frac{A}{2}-Z\right]^2 A^{-1}+a_P \delta A^{-1/2}+$$

$$a_6\ |A-252|\|A-a_7||N-152|1N+a_8|N-Z-50|/A$$

in the decay process of ^{286}112and other super heavy nuclei .The inclusion of these effects might resolve the issue related to island of stability in super heavy region.

3.3 References:

[1] Oganessian Yu Ts et al 2004, Phys. Rev. C 70 064609

[2] Island of stability for super heavy elements and dynamical cluster decay model for fusion evaporation residues cross-section: $_{20}Ca^{48}$ +42U238⟶112Uub286, J. Phys. G: Nucl. Part. Phys. 36 (2009) 115105 (15pp), Department of Physics, Punjab University, Chandigarh 160 014, India

[3] Myers W and Swiatecki's W J 1966 Nucl. Phys. 81 1

[4] Cwiok S, Dobaczewski J, Heenen P-H, Magierski P and Nazarewicz W 1996 Nucl. Phys. A 611 211, Cwiok S, Nazarewicz W and Heenen P H 1999 Phys. Rev. Lett. 83 1108.

[5] Kruppa A T, Bender M, Nazarewicz W, Reinhard P-G, Vertse T and Cwiok S 2000 Phys. Rev. C 61 034313.

[6]T. Dong and Z. Ren, Eur. Phys. J. A 26, 69 (2005).W. Nazarewic, Nucl.Phys.A611, 211(1996).